Assignments of ^{31}P NMR Resonances in Oligodeoxyribonucleotides: Origin of Sequence-Specific Variations in the Deoxyribose Phosphate Backbone Conformation and the ^{31}P Chemical Shifts of Double-Helical Nucleic Acids†

David G. Gorenstein,* Stephen A. Schroeder, Josepha M. Fu, James T. Metz, Vikram Roongta, and Claude R. Jones

Department of Chemistry, Purdue University, West Lafayette, Indiana 47907

Received February 12, 1988; Revised Manuscript Received April 29, 1988

ABSTRACT: It is now possible to unambiguously assign all ^{31}P resonances in the ^{31}P NMR spectra of oligonucleotides by either two-dimensional NMR techniques or site-specific ^{17}O labeling of the phosphoryl groups. Assignment of ^{31}P signals in tetradecamer duplexes, $(dTGTGAGCGCTCACA)_2$, $(dTATGAGCGCTCATA)_2$, $(dTCTGAGCGCTCAGA)_2$, and $(dTGTGTGCGCACACA)_2$, and the dodecamer duplex $d(CGTGAATTCGCG)_2$ containing one base-pair mismatch, combined with additional assignments in the literature, has allowed an analysis of the origin of the sequence-specific variation in ^{31}P chemical shifts of DNA. The ^{31}P chemical shifts of duplex B-DNA phosphates correlate reasonably well with some aspects of the Dickerson/Calladine sum function for variation in the helical twist of the oligonucleotides. Correlations between experimentally measured P–O and C–O torsional angles and results from molecular mechanics energy minimization calculations show that these results are consistent with the hypothesis that sequence-specific variations in ^{31}P chemical shifts are attributable to sequence-specific changes in the deoxyribose phosphate backbone. The major structural variation responsible for these ^{31}P shift perturbations appears to be P–O and C–O backbone torsional angles which respond to changes in the local helical structure. Furthermore, ^{31}P chemical shifts and $J_{H3'-P}$ coupling constants both indicate that these backbone torsional angle variations are more permissive at the ends of the double helix than in the middle. Thus ^{31}P NMR spectroscopy and molecular mechanics energy minimization calculations appear to be able to support sequence-specific structural variations along the backbone of the DNA in solution.

It is now widely appreciated that duplex DNA can exist in a number of different conformations (Saenger, 1984). Significant conformational differences can exist globally along the entire double helix, as in the A, B, C, and Z forms of DNA (Saenger, 1984). In addition, local conformational heterogeneity in the deoxyribose phosphate backbone has been most recently noted in the form of sequence-specific variations (Calladine, 1982; Dickerson, 1983; Dickerson & Drew, 1981, 1983) or as the result of drug (Saenger, 1984) or protein binding (Anderson et al., 1985; Hochschild & Ptashne, 1986; Martin & Schleif, 1986; McClarin et al., 1986; Richmond et al., 1985) to local regions of the DNA.

It has been suggested that these localized, sequence-specific conformational variations are quite likely an important component of a DNA binding protein's recognition of specific sites on the DNA (Dickerson, 1983; Dickerson & Drew, 1983; Gorenstein et al., 1987). Thus, although the *lac* repressor protein does not recognize an alternating AT sequence as part of the *lac* operator DNA sequence, the repressor protein binds to poly[d(AT)] 1000 times more tightly than to random DNA (Riggs et al., 1972; Saenger, 1984). The repressor protein is quite likely recognizing the alternating deoxyribose phosphate backbone geometry of the two strands, (Klug et al., 1979) rather than the chemical identity of the AT base pairs. Indeed, a recent X-ray crystallographic study (Anderson et al., 1987) on a related repressor–DNA complex shows that much of the specificity of the protein for the operator-DNA sequence is provided by protein contacts with the *phosphates*, and it is the sequence-specific variation in the conformation of the deoxyribose phosphate backbone that provides much of the operator-DNA specificity.

While X-ray crystallography has provided much of our understanding of these DNA structural variations, increasingly, high-resolution NMR has also begun to provide detailed three-dimensional structural information on duplex oligonucleotides (Broido et al., 1984; Feigon et al., 1983a,b; Frechet et al., 1983; Hare et al., 1983; James, 1984; Kearns, 1984; Lai et al., 1984; Scheek et al., 1984; Schroeder et al., 1987, 1986; Shah et al., 1984b). Unfortunately, of the six torsional angles that largely define the backbone structure, only the four involving the deoxyribose ring have been shown to be directly amenable to analysis by NMR techniques. In fact for modest-sized oligonucleotide duplexes, determination of these torsional angles through measurement of three-bond coupling constants is very difficult. Using the time development of cross-peak intensities in 2D-NOESY NMR spectra, a number of workers (Broido et al., 1984; Feigon et al., 1983a,b; Frechet et al., 1983; Hare et al., 1983; Lai et al., 1984; Scheek et al., 1984; Schroeder et al., 1986; Shah et al., 1984b) have been able to qualitatively or semiquantitatively determine whether two protons are within 5 Å of each other. From these NOESY-derived distances and restrained molecular dynamics (Nilges et al., 1987a,b) or distance geometry (Hare et al.,

† Supported by NIH (GM36281), the Purdue University Biochemical Magnetic Resonance Laboratory which is supported by NIH (Grant RR01077 from the Biotechnology Resources Program of the Division of Research Resources), and the NSF National Biological Facilities Center on Biomolecular NMR, Structure and Design at Purdue (Grants BBS 8614177 and BBS 8714258 from the Division of Biological Instrumentation). Support by the John Simon Guggenheim Memorial Foundation for a fellowship to D.G.G. is also gratefully acknowledged.

* Address correspondence to this author.

0006-2960/88/0427-7223$01.50/0

FIGURE 1: Conformations g,t (right) and g^-,g^- (left). Dihedral angles about the $(R)O_1$–P and $(R)O_2$–P bonds are defined by the R–O_1–P—O_2–R structural fragment and are gauche (g, dihedral angle 60°) are trans (t, dihedral angle 180°).

1986; Wemmer & Reid, 1985) calculations, models for these duplexes may be determined. While base pairing and stacking interactions can often be adequately demonstrated, detailed sequence-specific conformational information, especially with regard to the deoxyribose phosphate backbone, is often lacking.

Until recently (Lefevre et al., 1987; Nilges et al., 1987a,b), NMR spectroscopy has not been particularly successful in defining these potentially significant sequence-specific variations in the local conformation of the DNA (Assa-Munt & Kearns, 1984; Clore et al., 1985; Patel et al., 1983, 1987; Rinkel et al., 1987). Indeed, a recent ^1H NMR study of a duplex decamer failed to reproduce sequence-specific variations in the sugar ring conformation predicted by X-ray crystal analysis (Rinkel et al., 1987). Molecular mechanics and dynamics theoretical calculations (Kollman et al., 1982; Levitt, 1978; Singh, 1985) have also failed to reproduce these variations and have raised the question whether the sequence-specific structural variations observed in the X-ray crystallographic studies are the result of less profound crystal packing forces.

Previous efforts to establish sequence-specific variations in the *backbone* conformation of oligonucleotides have generally not been successful (Dickerson, 1983; Fratini et al., 1982). In this paper we wish to demonstrate that ^{31}P NMR spectroscopy can provide a powerful probe of these sequence-specific structural variations in solution. ^{31}P NMR and molecular mechanics energy minimization calculations are thus shown to support these sequence-specific variations along the backbone of the DNA.

Stereoelectronic Effect on ^{31}P Chemical Shifts as a Probe of DNA Structure. We have noted that ^{31}P chemical shifts can potentially provide a probe of the conformation of the phosphate ester backbone in nucleic acids and nucleic acid complexes (Gorenstein, 1978, 1981, 1984; Gorenstein & Findlay, 1976; Gorenstein & Goldfield, 1984; Gorenstein et al., 1987). Molecular orbital calculations in our laboratory provided initial suggestions that ^{31}P chemical shifts were influenced by conformation-dependent orbital interactions which we have ascribed to a stereoelectronic effect (Gorenstein, 1987). These and later calculations (Gorenstein, 1983; Gorenstein & Kar, 1975) suggested that the ^{31}P resonance of a phosphate diester in a g,g conformation should be several ppm upfield of the ^{31}P signal of an ester in a g,t or t,t conformation (Figure 1) (Gorenstein, 1984). Pullman and coworkers (Giessner-Prettre et al., 1984; Ribas-Prado et al., 1979) have confirmed our earlier calculations of the isotropic ^{31}P chemical shifts with much more reliable gauge invariant ^{31}P chemical shielding tensor and isotropic chemical shift calculations.

These initial theoretical calculations, as well as some simple model (Gorenstein, 1981) studies, suggested that we might be able to use this stereoelectronic effect on ^{31}P chemical shifts as a probe of nucleic acid conformations. Thus, as described above, if ^{31}P chemical shifts are sensitive to phosphate ester conformations, they potentially provide information on two of the most important torsional angles that define the nucleic acid deoxyribose phosphate backbone. One of these, the C3′–O3′—P–O5′ torsional angle ζ, is also found to be the most variable one in the B form of the double helix, and the other, O3′–P—O5′–C5′ torsional angle α, is one of the most variable in the A form of the duplex (Saenger, 1984). Indeed, following the original suggestion of Sundaralingam (1969) and on the basis of recent X-ray crystallographic studies of oligonucleotides, Saenger (1984) has noted that the P–O bonds may be considered the "major pivots affecting polynucleotide structure".

Variation of ^{31}P Chemical Shifts in Oligonucleotides. Earlier ^{31}P NMR studies on poly- and oligonucleic acid (Gorenstein et al., 1976; Gorenstein & Kar, 1975; Patel, 1979, 1974) supported our suggestion that the base-stacked, helical structure with a gauche,gauche phosphate ester torsional conformation should be upfield from the random coil conformation, which contains a mixture of phosphate esters in other non-gauche conformations as well. More recently, we (Gorenstein et al., 1986; Lai et al., 1984; Schroeder et al., 1986; Shah et al., 1984a,b) and others (Petersheim et al., 1984; Connolly & Eckstein, 1984; Ott & Eckstein, 1985a,b) have used a ^{17}O- or $^{17}O/^{18}O$-labeling scheme to identify the individual ^{31}P resonances of oligonucleotides. These labeling studies have allowed us to gain insight into the variou factors responsible for ^{31}P chemical shift variations in oligonucleotides (Cheng et al., 1987, 1982; Lai et al., 1984; Ott & Eckstein, 1985b; Patel, 1974b, 1979; Schroeder et al., 1986; Shah et al., 1984a,b). As discussed above, one of the major contributing factors that we have hypothesized determines ^{31}P chemical shifts is the main chain torsional angles of the individual phosphodiester groups along the oligonucleotide double helix. Phosphates located toward the middle of a B-DNA double helix assume the lower energy, stereoelectronically (Gorenstein, 1987) favored g^-,g^- conformation, while phosphodiester linkages located toward the two ends of the double helix tend to adopt a mixture of g^-,g^-, t,g^-, and g^-,t conformations, where increased flexibility of the helix is more likely to occur. [The notation for the P–O ester torsion angles follows the convention of Seeman et al. (1976) with the ζ, P–O3′, angle given first followed by the α, P–O5′, angle.] Because the g^-,g^- conformation is responsible for a more upfield ^{31}P chemical shift, while a g^-,t or t,g^- conformation is associated with a lower field chemical shift, internal phosphates in oligonucleotides would be expected to be upfield of those nearer the ends. Although several exceptions have been observed, this positional relationship appears to be generally valid for oligonucleotides where ^{31}P chemical shift assignments have been determined (Gorenstein, 1978; Gorenstein et al., 1976; Ott & Eckstein, 1985a,b; Petersheim et al., 1984; Schroeder et al., 1987, 1986). Thus, position of the phosphorus (terminal vs internal) within the oligonucleotide is one important factor responsible for variations in ^{31}P chemical shifts.

Learner and Kearns (1980), however, have shown that ^{31}P chemical shifts of phosphate esters are modestly sensitive to solvation effects and have argued that differential solvation of the nucleic acid phosphates could be responsible for the observed variation in the ^{31}P chemical shifts of nucleic acids. Costello et al. (1976) have also noted similar sensitivity of ^{31}P chemical shifts to salt. As argued in this paper, it appears as though these environmental effects on the ^{31}P chemical shifts of nucleic acids are smaller than the intrinsic conformational factors discussed above, assuming comparisons are made under similar solvation conditions. Similarly, other possible effects, such as ring-current shifts, are not likely to be responsible for

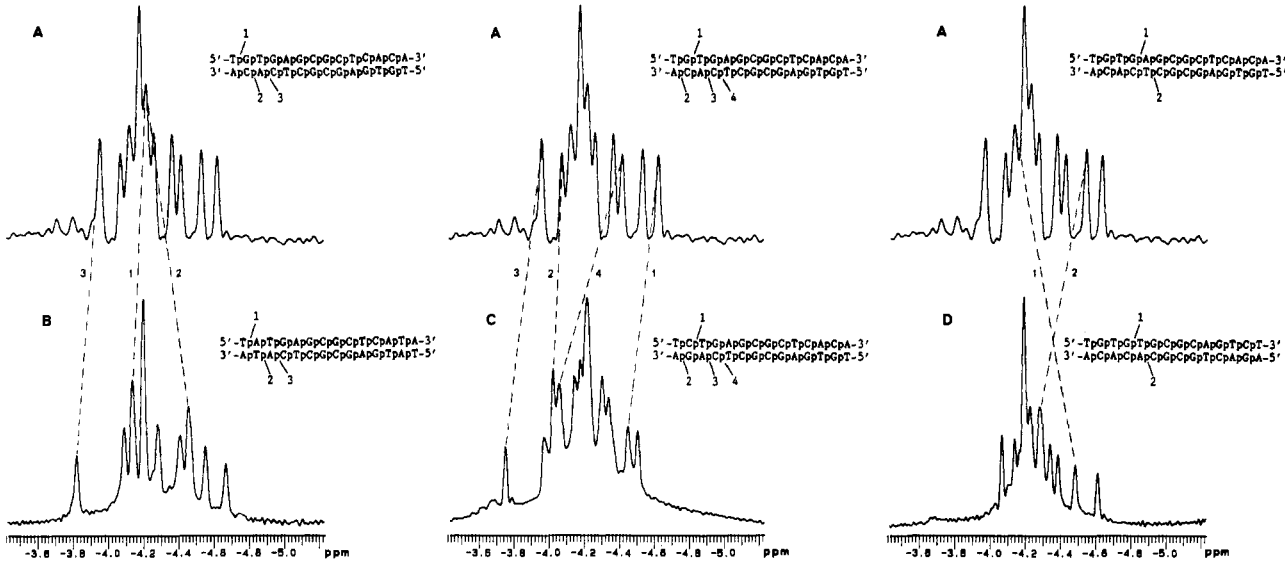

FIGURE 2: ^{31}P NMR spectra of (A) 14-mer **1**, (B) 14-mer **2**, (C) 14-mer **3**, and (D) 14-mer **4**. Samples contained 4–6 mg of purified 14-mers in 0.4 mL of D_2O containing 25 mM Hepes, 10 mM EDTA, 75 mM KCl, and 0.1 mM NaN_3, pH* 8.0 (uncorrected pH meter reading in D_2O).

shifts >0.01 ppm (Giessner-Prettre et al., 1976; Gorenstein, 1984). The latter effects are so small because the phosphates are so far removed from the bases (>10 Å). Bond angle distortions can have a large effect on ^{31}P chemical shifts (Giessner-Prettre et al., 1984; Gorenstein, 1984; Gorenstein & Kar, 1977), but this geometric parameter is coupled to the torsional angle changes (Gorenstein et al., 1977) so it is not an independent variable.

Eckstein and co-workers (Connolly & Eckstein, 1984; Ott & Eckstein, 1985a,b) have recently noted that the occurrence of a 5′-pyrimidine–purine-3′ base sequence (5′-PyPu-3′) within the oligonucleotide has a more downfield than expected ^{31}P chemical shift if based solely on the phosphate positional relationship. They have suggested an explanation for these anomalous chemical shifts based upon sequence-specific structural variations of the double helix as proposed by Calladine (1982). As described in more detail below, local helical distortions arise along the DNA chain due to purine–purine steric clash on opposite strands of the double helix (Calladine, 1982). As a result, 5′-PyPu-3′ sequences within the oligonucleotide represent positions where the largest helical distortions occur. Eckstein and co-workers have proposed, on the basis of the ^{31}P assignments of two dodecamers and an octamer, that a correlation exists between the helical roll angle parameter (Calladine, 1982; Dickerson, 1983) and ^{31}P chemical shifts (Ott & Eckstein, 1985a,b). They have noted a considerably poorer correlation between ^{31}P chemical shifts of the oligonucleotides and other sequence-specific variations in duplex geometry (such as the helix twist; see below). In this paper we wish to analyze these sequence-specific variations in the ^{31}P chemical shifts and conformation of duplex DNA. The ^{31}P data and molecular mechanics calculations will be shown to provide support both for the Calladine rules and for the torsional angle effect on ^{31}P chemical shifts.

Experimental Procedures

Synthesis and Sample Preparation. The self-complementary tetradecamers d(TGTGAGCGCTCACA) (**1**), d(TATGAGCGCTCATA) (**2**), d(TCTGAGCGCTCAGA) (**3**), and d(TGTGTGCGCACACA) (**4**), the GT-12-mer d(CGTGAATTCGCG) (**5**), and the GC-12-mer d(CGCGAATTCGCG) (**6**) were synthesized by a manual modification of the phosphite triester method on a solid support as previously described (Lai et al., 1984; Schroeder et al., 1987; Shah et al., 1984b,c). We have introduced the ^{17}O label into the phosphoryl group by replacing the I_2/H_2O in the oxidation step of the phosphite by $I_2/H_2{}^{17}O$ (Monsanto $H_2{}^{17}O$: 51.5% ^{17}O, 35.6% ^{18}O, 12.9% ^{16}O) as previously described (Lai et al., 1984; Shah et al., 1984b,c) [see also Petersheim et al. (1984) and Eckstein and co-workers (Ott and Eckstein, 1985a,b)]. After cleavage from the support and deprotection, the resulting oligonucleotides were purified by reversed-phase HPLC (Schroeder et al., 1987) followed by dialysis.

^{31}P NMR samples contained 4–6 mg of purified 14-mers in 0.4 mL of D_2O containing 25 mM Hepes, 10 mM EDTA, 75 mM KCl, and 0.1 mM NaN_3, pH* 8.0.

NMR. The ^{31}P NMR spectra were performed on a Varian XL-200A (200 MHz ^{1}H) spectrometer at ambient temperature. ^{31}P NMR parameters were as follows: sweep width 172 Hz; acquisition time 2.98 s; block size 1K zero filled to 16K; pulse width 7.0 μs. Spectra were resolution enhanced with a combination of positive exponential and Gaussian apodization functions; the number of acquisitions was between 2000 and 3000. The resulting spectra are presented in Figures 2 and 3. ^{31}P NMR resonances are referenced to an external sample of trimethyl phosphate (TMP), which is 3.53 ppm downfield of 85% H_3PO_4. Assignments of the individual signals to the phosphates of the duplex were accomplished by either site-specific ^{17}O labeling of the phosphoryl groups [14-mer **1** (Schroeder et al., 1987) and 12-mer **5**, as described in this paper] or a combination of ^{1}H signal assignments from 2D ^{1}H/^{1}H NOESY and COSY followed by heteronuclear ^{1}H/^{31}P correlation *P*ure *A*bsorption-phase *C*onstant time (PAC) spectra (Fu et al., 1988) (oligonucleotides **2**–**4**).

Molecular Mechanics Calculations. The NUCGEN module of the program AMBER (Weiner & Kollman, 1981) was used to generate a series of idealized Arnott B-DNA dinucleoside monophosphate duplex structures with the sequence d(TG)·d(CA) (Figure 4) in which the helix twist was varied from 25° to 45° while the helical height was kept fixed at 3.38 Å. The model-built structures were then energy refined until a rms gradient of 0.1 kcal/(mol·Å) was achieved or until the change in energy was less than 1.0×10^{-7} kcal/mol for successive steps. The four C4′ atoms were constrained in all structures (force constant 9999.99 kcal mol^{-1} Å^2) except for a control duplex with a model-built helix twist of 36.0°.

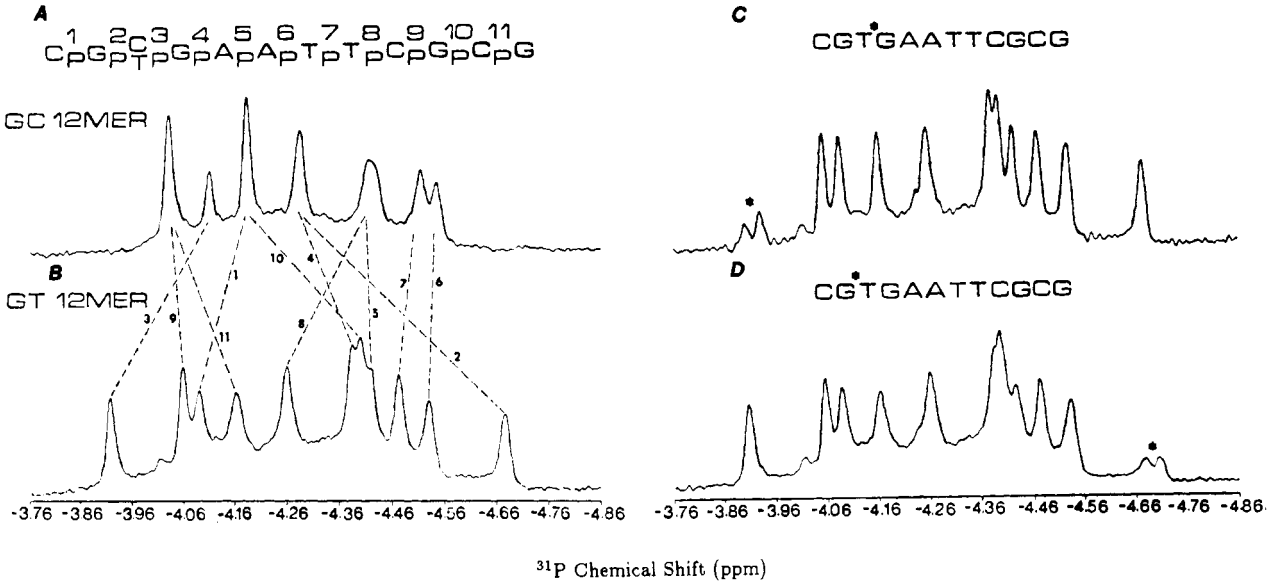

FIGURE 3: ^{31}P NMR spectra and phosphate assignments of (A) GC-12-mer **6** [assignments from Ott and Eckstein (1985a)] and (B) GT-12-mer **5**. (Numbering corresponds to phosphate position from the 5′ end of the duplexes). Examples of site-specific ^{17}O labeling of two of the phosphates of GT-12-mer **5** at positions 3 and 2 (shown by an asterisk) are shown in (C) and (D), respectively.

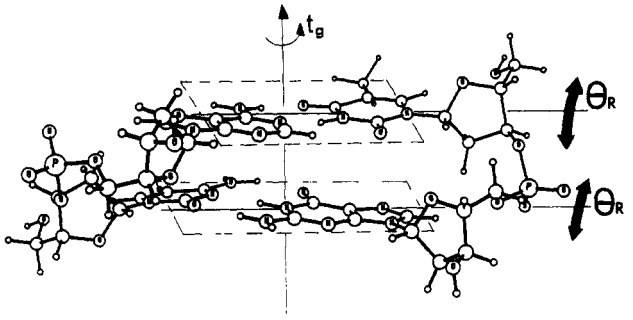

FIGURE 4: Model of d(TpG)·d(CpA) showing definition of helix twist, t_g, and helix roll (θ). Dickerson (1983) defines t_g as the angle of the C1′–C1′ vectors in two successive base pairs, viewing the duplex down along the best overall helix axis. In our own calculations we have followed the AMBER definition (Weiner et al., 1986) based upon the interstrand C1′–C1′ vectors. Helix roll, θ, is defined (Dickerson, 1983) as the change in the orientation of the best planes of successive base pairs along their long axes.

RESULTS

Assignment of ^{31}P Signals of Oligonucleotide Duplexes **1–5**. Using the solid-phase phosphoramidite method, we have synthesized deoxyoligonucleotides **1–5**. Assignment of the ^{31}P signals was accomplished by either 2D NMR (Fu et al., 1988; Schroeder et al., 1987; Sklenář et al., 1986) or ^{17}O-labeling methodologies (Schroeder et al., 1987). 14-mers **2–4**, which differ by a single base-pair change from 14-mer **1**, have been assigned by a PAC 2D heteronuclear correlation NMR method (Fu et al., 1988). The ^{31}P chemical shift variations from one base step to the next for each of the three 14-mer single base-pair "mutant" sequences **2–4** as compared to those of the 14-mer **1** sequence are shown in Figure 2. In general, the ^{31}P shifts of phosphate positions at or within two adjacent positions to the site of mutation are affected, while positions at identical base steps are associated with equivalent ^{31}P shifts. Note, however, that the ^{31}P chemical shifts within the central portion of 14-mer **3**, that is, the ^{31}P shift variation from one base step to the next, are significantly different, suggesting, as discussed below, that the helical nature within the central portion of the sequence is altered with respect to that of the 14-mer **1** sequence.

dTGTGAGCGCTCACA
dACACTCGCGAGTGT
1
dTATGAGCGCTCATA
dATACTCGCGAGTAT
2
dTCTGAGCGCTCAGA
dAGACTCGCGAGTCT
3
dTGTGTGCGCACACA
dACACACGCGTGTGT
4
dCGTGAATTCGCG
dGCGCTTAAGTGC
5

^{31}P signals of oligonucleotide **5** were assigned by the ^{17}O-labeling methodology. We can readily introduce ^{17}O labels into the phosphoryl groups by replacing the I_2/H_2O in the oxidation step of the phosphite by $I_2/H_2{}^{17}O$ (40%) (Schroeder et al., 1987; Shah et al., 1984b). By synthesizing a mono-[^{17}O]phosphoryl-labeled oligonucleotide (one specific phosphate is labeled along the strand), we can identify the ^{31}P signal of that phosphate diester. This is because the quadrupolar ^{17}O nucleus (generally ca. 40% enriched) broadens the ^{31}P signal of the directly attached phosphorus to such an extent that only the high-resolution signal of the remaining 60% nonquadrupolar broadened phosphate at the labeled site is observed (Connolly & Eckstein, 1984; Petersheim et al., 1984; Shah et al., 1984b). In this way each synthesized oligonucleotide with a different monosubstituted [^{17}O]phosphoryl group allows identification of one specific ^{31}P signal, and the full series of monolabeled oligonucleotides gives the assignment of the entire ^{31}P NMR spectrum.

Figure 3 shows representative ^{31}P spectra of unlabeled and singly ^{17}O-labeled GT-12-mers **5**. Figure 3B is a spectrum of the GT-12-mer **5** without any ^{17}O label that can be used as a comparison between labeled spectra. As can be seen in spectra C and D of Figure 3, a decrease in intensity of a single

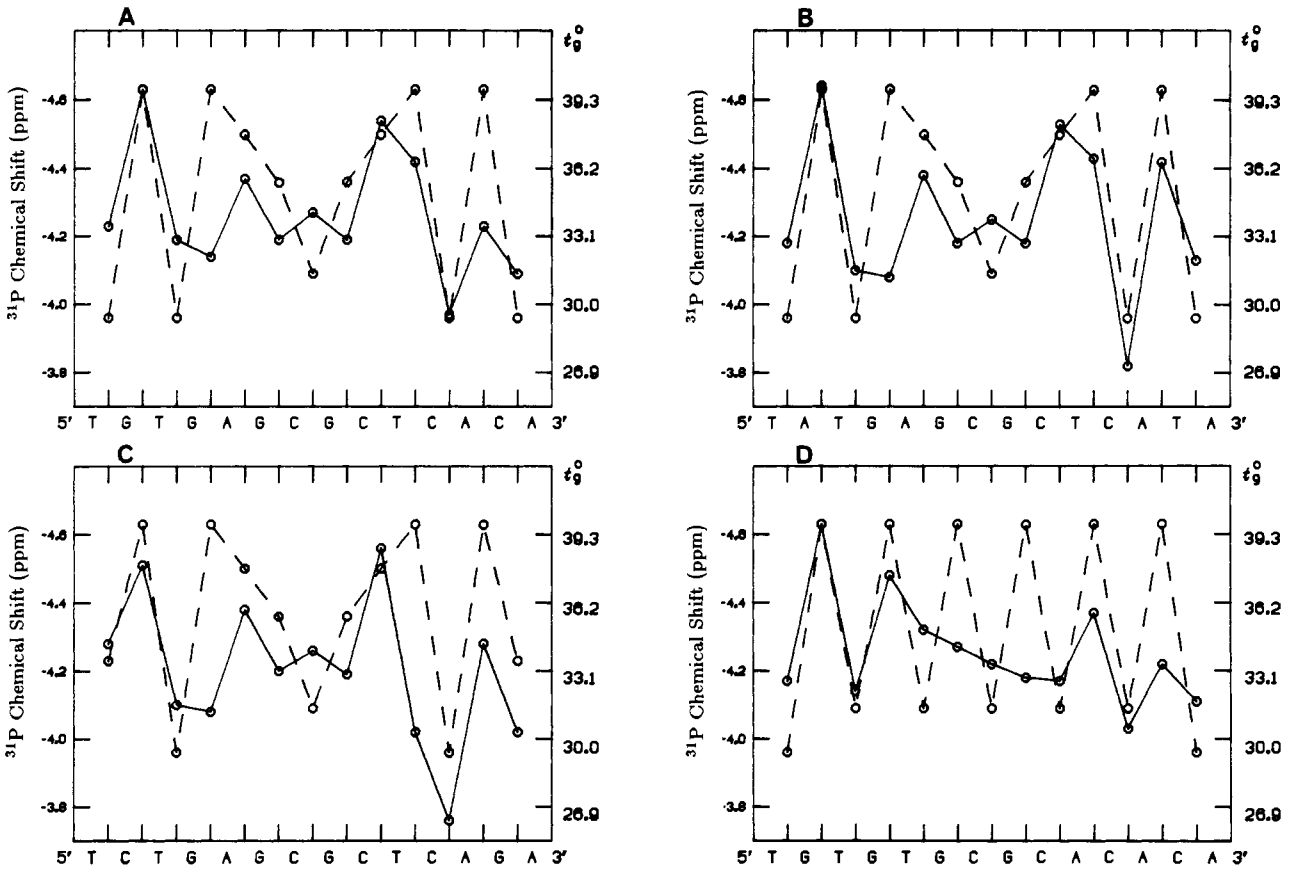

FIGURE 5: Plot of ^{31}P chemical shift (O—O) vs phosphate position along the 5′–3′ strand for duplex (A) 14-mer **1**, (B) 14-mer **2**, (C) 14-mer **3**, and (D) 14-mer **4**. Also shown is a plot of calculated helix twist sum, t_g, derived from the calculated $\sum_1$ sum function and eq 1 ($t_g = 35.6 + 2.1\sum_1$) vs phosphate position (O--O). The t_g vs sequence plot has been scaled to reflect the ^{31}P chemical shift variations.

resonance is observed. All 11 resonances can clearly be distinguished, each integrating for 1 phosphorus resonance. It is interesting to note that the resonance of the labeled phosphate is observed as two reduced-intensity, resolved peaks associated with ^{16}O (unlabeled) and ^{18}O-labeled phosphorus resonances. (The $H_2{}^{17}O$ sample also contains both $H_2{}^{16}O$ and $H_2{}^{18}O$; see Experimental Procedures.) This can most easily be seen in spectra C and D of Figure 3 where the ^{18}O-labeled phosphate ^{31}P signal is shifted slightly upfield relative to the remaining ^{16}O phosphate phosphorus resonance (Shah et al., 1984b).

Patel et al. (1982) have shown that base-pair mismatch in duplex **5** provides some very interesting ^{31}P spectral shifts. Whereas the ^{31}P spectral dispersion is generally <0.6 ppm in normal B-DNA double helices (as seen in the spectra of Figure 2 for duplex oligonucleotides **1**–**4**), new signals are shifted upfield and downfield from the "normal" double-helical phosphate ^{31}P signals in duplex **5**. A comparison of the ^{31}P resonance assignments for the Dickerson base-paired GC-12 mer d(CGCGAATTCGCE)$_2$ (**6**), and the GT-mismatch 12-mer **5** [the GC-12-mer assignments are from Eckstein and co-workers (Ott & Eckstein, 1985a)] is also shown in spectra A and B of Figure 3.

In general, the ^{31}P chemical shifts of those phosphates in GT-12-mer **5** furthest from the mismatch sites at position 3 from both 5′ ends of the duplex are quite similar to those of GC-12-mer **6**. The two signals shifted the most upfield (GpT phosphate at position 2) and downfield (TpG phosphate at position 3) occur at the site of mismatch.

Comparison of ^{31}P Chemical Shifts of Other Oligonucleotides. To date, only nine "modest"-sized oligonucleotide sequences have had individual ^{31}P resonances completely assigned. All are self-complementary (or nearly self-complementary) sequences:

1-5

dCGCGAATTCGCG

dGCGCTTAAGCGC

6

dGACGATATCGTC

dCTGCTATAGCAG

7

dCATG—G—AT(5-MeC)CATG

dGTAC(5-MeC)TA—G—GTAC

8

dGGAATTCC

dCCTTAAGG

9

The individual ^{31}P chemical shifts of oligonucleotides duplexes **1**–**9** (referenced to trimethyl phosphate, 0 ppm) are shown in Table I and are plotted vs sequence in Figures 5 and 6. Three of the sequences were assigned by Eckstein and co-workers using ^{17}O labeling, and these are designated GC-12-mer **6** (Ott & Eckstein, 1985a), 12-mer **7** (Ott & Eckstein, 1985b), and 8-mer **9** (Connolly & Eckstein, 1984). [The two dodecamer sequences, GC-12-mer **6** and 12-mer **7**, were initially selected on the basis that these two sequences contain recognition sites for restriction endonucleases *Eco*RI and *Eco*RV, respectively. In addition, crystal structure analysis of the sequence-specific helical variations in GC-12-mer **6** led to the formation of the Calladine rules and sum function relationships (Calladine, 1982; Dickerson, 1983; Dickerson &

Table I: ^{31}P Chemical Shifts (ppm) of Oligonucleotides **1–9**

1	^{31}P shift	**2**	^{31}P shift	**3**	^{31}P shift	**4**	^{31}P shift	**5**	^{31}P shift	**6**	^{31}P shift	**7**	^{31}P shift	**8**	^{31}P shift	**9**	^{31}P shift
T	−4.23	T	−4.10	T	−4.28	T	−4.17	C	−4.08	C	−4.18	G	−4.25	C	−4.02	G	−4.04
G	−4.63	A	−4.64	C	−4.51	G	−4.63	G	−4.67	G	−4.28	A	−4.40	A	−4.47	G	−4.13
T	−4.19	T	−4.18	T	−4.10	T	−4.14	T	−3.46	C	−4.07	C	−4.01	T	−4.10	A	−4.37
G	−4.14	G	−4.08	G	−4.08	G	−4.48	G	−3.90	G	−4.32	G	−4.26	G	−3.85	A	−4.49
A	−4.37	A	−4.38	A	−4.38	T	−4.32	A	−4.41	A	−4.42	A	−4.48	G	−4.19	T	−4.43
G	−4.19	G	−4.18	G	−4.20	G	−4.27	A	−4.52	A	−4.54	T	−4.34	A	−4.37	T	−4.22
C	−4.27	C	−4.25	C	−4.26	C	−4.22	T	−4.46	T	−4.51	A	−4.51	T	−4.33	C	−3.87
G	−4.19	G	−4.18	G	−4.19	G	−4.18	T	−4.25	T	−4.42	T	−4.32	C	−4.13	C	
C	−4.54	C	−4.53	C	−4.56	C	−4.17	C	−4.05	C	−4.05	C	−4.01	C	−3.84		
T	−4.42	T	−4.43	T	−4.02	A	−4.37	G	−4.39	G	−4.18	G	−4.40	A	−4.37		
C	−3.97	C	−3.82	C	−3.76	T	−4.03	C	−4.15	C	−4.02	T	−4.07	T	−4.05		
A	−4.23	A	−4.42	A	−4.28	A	−4.22	G		G		C		G			
C	−4.09	T	−4.13	G	−4.02	T	−4.11										
A		A		A		A											

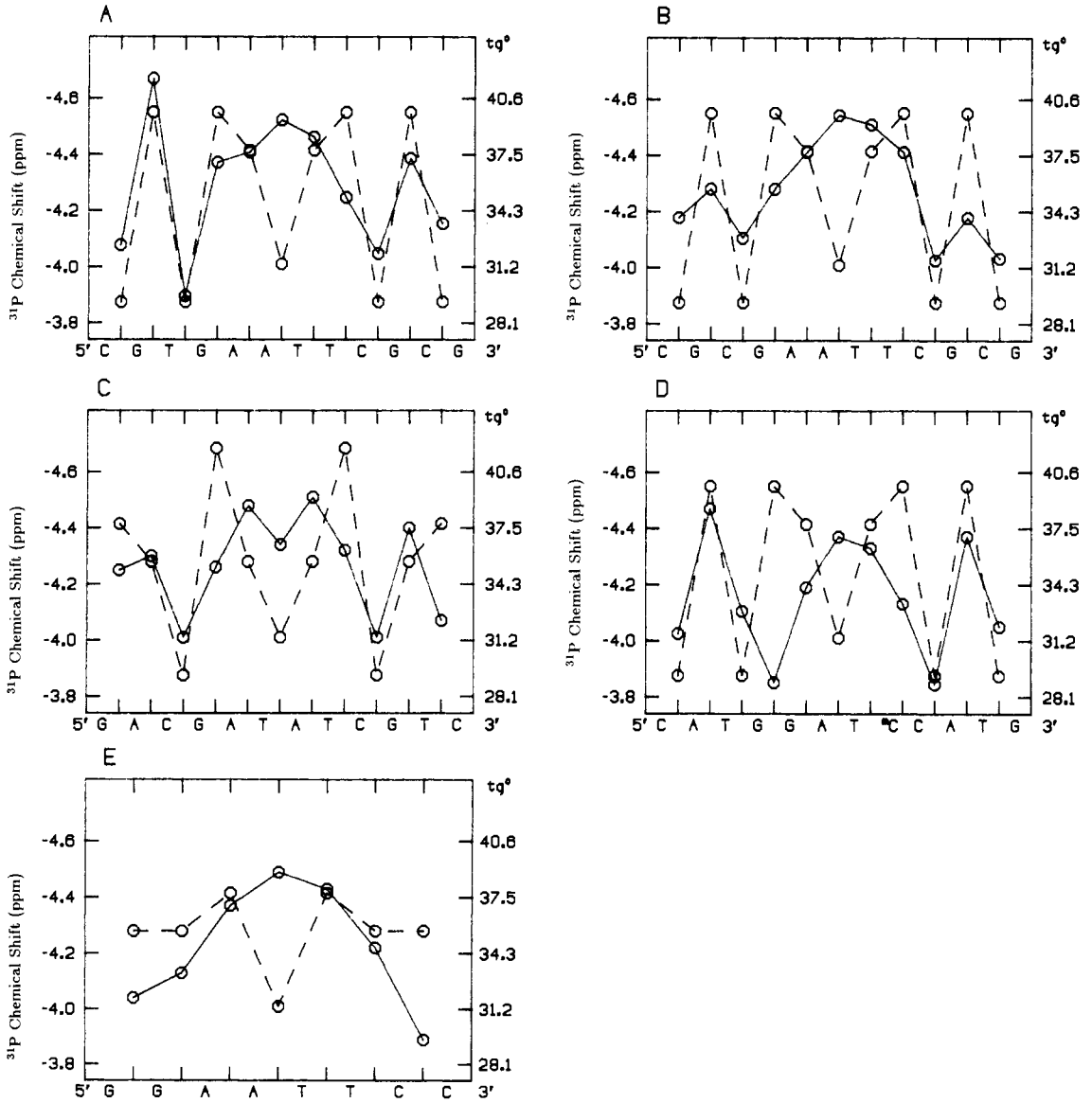

FIGURE 6: Plot of ^{31}P chemical shift (O—O) vs phosphate position along the 5′–3′ strand for duplex (A) GT-12-mer **5**, (B) GC-12-mer **6**, (C) 12-mer **7**, (D) 12-mer **8**, and (E) 8-mer **9**. Also shown is a plot of calculated helix twist sum, t_g, derived from the calculated $\sum_1$ sum function and eq 1 ($t_g = 35.6 + 2.1\sum_1$) vs phosphate position (O--O). The t_g vs sequence plot has been scaled to reflect the ^{31}P chemical shift variations.

Drew, 1983).] Bax and co-workers have assigned the ^{31}P resonances of the dodecamer **8** using inverse detection ^{31}P–^{1}H HETCOR (Sklenář et al., 1986). The other sequences, the 14-mer sequence **1** (Schroeder et al., 1987) and the GT-dodecamer **5**, were also assigned by ^{17}O labeling, while "mutant" 14-mers **2–4** were assigned by a PAC 2D heteronuclear correlation NMR method (Fu et al., 1988) and were carried out in our laboratory [14-mer **1** assignments were also confirmed by the PAC 2D NMR method]. Note that GT-12-mer **5** is identical in base sequence with the Dickerson 12-mer **6** sequence except that it contains a GT base-pair mismatch at the third position from the end, which is expected to perturb the structure and possibly the ^{31}P chemical shifts at phosphates at or adjacent to this position. The 12-mer sequence **8** has

a methylcytosine residue at base position 8 which could perturb the helical structure. It was felt, however, that these sequences could still be included in the overall comparison in order to verify common trends in ^{31}P chemical shifts of the other sequences.

Sequence-Specific Variation in ^{31}P Chemical Shifts: Calladine Rules. As shown in Figures 5 and 6, with the exception of 8-mer **9**, the ^{31}P chemical shifts of the duplex oligonucleotides do not appear to uniformly follow the positional relationship. As would be expected from the phosphate positional relationship, the ^{31}P chemical shifts in the central regions should gradually increase, reach a maximum at the central phosphate position, and decrease once again, due to the favorable energetic considerations of the internucleotidic linkages for internal regions of the oligonucleotide. The central region of the GT-12-mer **5**, GC-12-mer **6**, 12-mer **8**, and 8-mer **9** sequences appears to follow the positional relationship. However, major variations which do not follow the positional relationship of ^{31}P chemical shifts are observed throughout the 12-mers and 14-mers.

As first suggested by Eckstein and co-workers, the ^{31}P chemical shifts appear to vary in response to local, sequence-specific distortions in the duplex geometry. The possible basis for the correlation between sequence-specific helical distortion and ^{31}P chemical shifts can be understood from the following geometrical analysis. Calladine (Calladine, 1982; Calladine & Drew, 1984) and Dickerson (Calladine, 1982; Dickerson, 1983; Fratini et al., 1982) analyzed the crystal structure of 12-mer **6** and suggested a simple mechanical explanation for the significant distortions from a regular B-DNA double-helical structure. It was noted that, in order to increase the stacking overlap along each strand of the double helix, the bases along each strand are propeller twisted by 10–20° relative to the bases on the opposite strand. Because the purines extend beyond the helix axis, in a 5′-purine–pyrimidine-3′ (5′-PuPy-3′) sequence or a 5′-PyPu-3′ sequence, the purines on opposite strands that are separated by one base step sterically clash. The purine N2/N3 steric clash in the minor groove of a 5′-PyPu-3′ sequence is twice as severe as the steric clash of the purines in the major groove of a 5′-PuPy-3′ sequence and hence a 5′-PyPu-3′ sequence produces the largest local geometry changes (Calladine, 1982; Dickerson, 1983; Dickerson & Drew, 1983). Using a simple elastic beam mechanical model, Calladine (1982; Calladine & Drew, 1984) has proposed four different conformational variations that will relieve this steric hindrance: (1) flattening the propeller twist, (2) opening the role angle, (3) displacing the base pairs, and (4) decreasing the local helix twist (Figure 4).

Because the origin of purine–purine cross-chain clash and subsequent methods of helical adjustment are inherently related to the purine–pyrimidine (or pyrimidine–purine) sequence, one would first want to compare common alternating purine/pyrimidine steps to see if any generalities in ^{31}P chemical shift patterns exist. Figures 5 and 6 compare the ^{31}P chemical shift pattern of each sequence. Common variations, and differences in ^{31}P chemical shifts between each sequence, can be expressed more clearly if separate comparisons are made between each of the internal regions and terminal regions of the oligonucleotides **1**–**9**.

Comparison of Terminal Regions. By mere coincidence five of the nine oligonucleotide sequences, GC-12-mer **6**, 12-mer **8**, and the 14-mers **1**, **2**, and **4**, have identical purine/pyrimidine terminal sequence for the first five base pairs, and thus one would initially expect the ^{31}P chemical shift patterns of

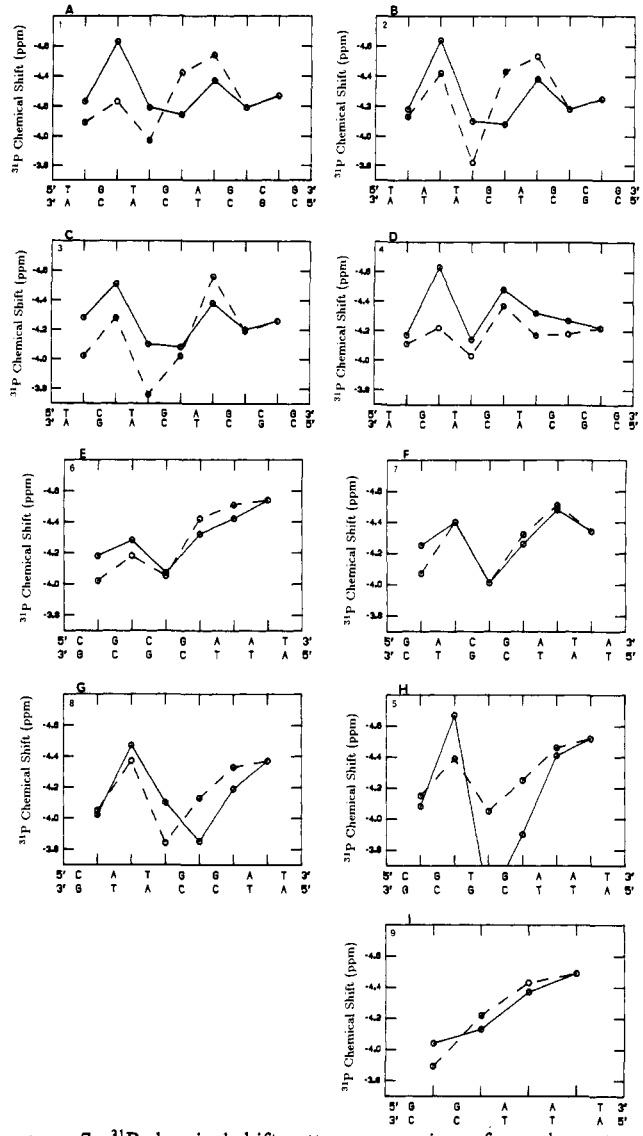

FIGURE 7: ^{31}P chemical shift pattern comparison of complementary phosphate positions in oligonucleotides **1**–**9**. Solid lines, 5′–3′ direction; dashed lines, complementary 3′–5′ direction.

each terminal region to be identical. It is important to note that the pattern of ^{31}P chemical shift variations at the ends of the two sequences of GT-12-mer **5** and 12-mer **7** are nearly identical with that occurring in the GC-12-mer **6**, 12-mer **8**, and 14-mer **1**–**4** sequences. This is exactly what is observed in each case, and thus one can conclude that the common variation in ^{31}P chemical shift within the two end regions is likely due to the same type of helical adjustment needed to relieve the purine–purine steric clash. These similarities thus strongly support the hypothesis that ^{31}P chemical shift variations arise from sequence-specific distortions in helix geometry.

Figure 7 compares ^{31}P chemical shifts for complementary positions for each of the eight duplex sequences, where the solid line connects ^{31}P chemical shifts for phosphate positions starting at the 5′ end and proceeding in the 3′ direction and the dashed line represents ^{31}P chemical shifts for the complementary 3′–5′ strand. Note that because of the palindromic symmetry of each of the oligonucleotides **1**–**9**, the corresponding phosphates on opposite strands that are related by the 2-fold dyad axis of symmetry are chemically and hence magnetically equivalent. However, the "complementary" phosphates (phosphates opposite each other on complementary strands) are chemically and magnetically nonequivalent.

Rather surprisingly, the ^{31}P chemical shifts at complementary phosphate positions generally follow the same pattern in both strands of the duplex regardless of base sequence or position, suggesting that the phosphate geometry is nearly the same in complementary positions along both strands.

As can be seen from the ^{31}P chemical shift pattern of the four phosphate positions shown in Figure 7, each minor groove clash step at phosphate position 3 is associated with a relative downfield ^{31}P chemical shift, while the adjacent major groove clash step at position 2 results in a large upfield ^{31}P chemical shift. (In the 12-mer **8** and the 14-mer **1** sequences phosphate position 2 has the most upfield ^{31}P chemical shift of all phosphates within the respective sequence. Also, it is interesting to note that the GT-12-mer **5** sequence also has the most upfield ^{31}P chemical shift at position 2, and thus this position may not be affected by the adjacent base pair mismatch.) The important point that is seen in Figure 7 is that while small differences in ^{31}P chemical shifts occur at common purine/pyrimidine steps, the ^{31}P chemical shift variation and absolute chemical shifts of each terminal-region phosphate are remarkably similar.

Since the actual base sequence that makes up the terminal regions is different in each of the sequences **1**–**9**, it would appear that the observed variation of ^{31}P chemical shifts is largely a function only of the purine/pyrimidine sequence. The through-space magnetic or electric chemical shielding effects of either a guanosine or adenosine base (i.e., through ring-current and electric charge effects) will not be identical at the phosphorus nucleus. The fact that it is immaterial whether an A or G base is present at a particular purine position in the sequence further supports the hypothesis that conformational differences arising from purine–purine clash are responsible for the ^{31}P chemical shift variations.

Still another common feature of the end-region ^{31}P chemical shift pattern deals with the large upfield ^{31}P chemical shift of phosphate position 2. This position is interesting in terms of suggested end effects where greater conformational flexibility (dynamic "fraying") of the double helix is more likely to occur. This, however, does not seem to be the case since significant end fraying would be expected to lessen the purine–purine clash. As a consequence the amount of helical adjustment necessary would be less at the corresponding clash positions at the ends of the duplex. The fact that position 2 has the most upfield ^{31}P chemical shift in each end region (and in some cases the most upfield ^{31}P chemical shift within a sequence) is consistent with this position being affected most by the purine–purine interaction and thus would imply that kinetic or thermodynamic fraying is less important. It should be kept in mind that a large upfield ^{31}P chemical shift is generally associated with a g^-,g^- phosphodiester conformation.

From the comparison of the ^{31}P chemical shifts of the end regions (Figures 5–7) two general conclusions can be made. First, oligonucleotide sequences with terminal regions having common purine–pyrimidine sequence will have very similar variations in ^{31}P chemical shift patterns. Second, a comparison of the ^{31}P chemical shift pattern shows that ^{31}P chemical shifts are still slightly affected by the actual base sequence. Therefore, it is still not possible to quantitatively predict ^{31}P chemical shifts of the phosphates in a given sequence.

^{31}P Chemical Shifts and Calladine Rules. Fratini et al. (1982) have shown that the helical distortions observed in the crystal structure of GC-12-mer **6** could be quantitatively predicted through a series of simple "Calladine rule" (Calladine, 1982) arithematic sum function relationships. Thus the global helical twist (t_g) can be calculated from eq 1 with the helical twist sum function ($\sum_1$).

$$t_g = 35.6° + 2.1\sum_1 \quad (1)$$

Dickerson (Dickerson, 1983; Fratini et al., 1982) has shown that when correction is made for some crystal packing distortions and end-for-end averaging is used, the linear regression correlation coefficient between the calculated t_g from eq 1 and the crystallographically observed helical twist is >0.9. Similar correlations have been established for base-plane roll angles, main-chain torsion angle δ, and propeller twist by use of $\sum_2$, $\sum_3$, and $\sum_4$ sum functions, respectively.

On the basis of the ^{31}P assignments of 14-mer **1**, we have previously suggested that there does appear to be a modest correlation between ^{31}P chemical shifts and the helical twist sum function for a number of the oligonucleotides (dashed line in Figures 5 and 6) (Schroeder et al., 1987, 1986). The correlation coefficient varies from a very poor value of −0.15 for the 8-mer **9** to a more respectable 0.74 for 12-mer **3**.

^{31}P chemical shift correlations with roll angle are quite similar to that observed for the helix twist (correlation coefficients vary from 0.17 for 14-mer **3** to 0.75 for oligomer **7**). Actually, the correlation of ^{31}P chemical shifts to helix twist is much better in the terminal regions and quite poor in the middle regions (in fact there is an anticorrelation). A modest improvement in the fit of ^{31}P chemical shifts to helix twist or roll angle is observed by eliminating the middle region positions in the correlations (see below).

Surprisingly, the GT-mismatch 12-mer duplex **5** also shows a good correlation between the helix twist sum function and the ^{31}P chemical shift (Figure 5, correlation coefficient 0.70). In contrast the normal GC-12 mer **6** does not show a very good correlation with this sum function (Ott & Eckstein, 1985a). Eckstein and co-workers have suggested that ^{31}P chemical shifts of the three sequences **6**, **7**, and **9** correlate best with the roll angle sum function (Connolly & Eckstein, 1984; Ott & Eckstein, 1985a,b). In fact, the ^{31}P chemical shifts of the GT-12-mer **5** also show a good correlation with the roll angle sum function (correlation coefficient of 0.81). Surprisingly, the two positions *least* expected to show these sorts of correlations (the two phosphates adjacent to the mismatch site) show very good correlations with the sum functions. This further substantiates the point that ^{31}P chemical shifts in these duplexes reflect in some way the local geometry of the duplex, independent of the exact chemical structure of the base.

If we do a least-squares fit of the assigned oligonucleotide ^{31}P shifts to the calculated helical twist (calculated from $\sum_1$ and eq 1), a rather modest correlation appears to exist between the two parameters. The correlation coefficient (R) between ^{31}P shifts and helical twist is 0.51–0.67 depending upon whether all of the ^{31}P shifts for all phosphates (R = 0.51) of oligonucleotides **1**–**9** or just those of the terminal phosphates are included in the correlation (R = 0.67). In the middle region, no correlation (R = 0.05) is found between ^{31}P chemical shifts and helix twist. If some drug–DNA ^{31}P chemical shifts are also included in the correlation between helix twist and end phosphate shifts, the correlation is slightly improved to 0.71 (Figure 8). Thus besides the ^{31}P chemical shifts of the terminal phosphates of the nine oligonucleotides, ^{31}P chemical shifts of several drug complexes are also included in Figure 8.

As pointed out by Jones and Wilson (1980), the ^{31}P chemical shifts of these drug complexes appear to correlate with the observed degree of unwinding of the duplex DNA upon drug binding. These downfield shifts of the ^{31}P signals have been ascribed to perturbations in the P–O ester torsion angles at the site of intercalation of the drug (Patel, 1974a,b, 1976,

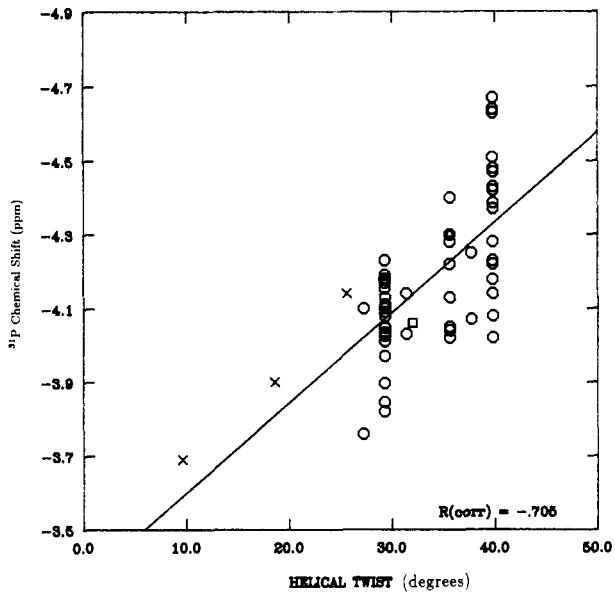

FIGURE 8: Plot of ^{31}P chemical shift vs calculated helix twist, t_g, derived from eq 1 ($t_g = 35.6 + 2.1\sum_1$). Oligonucleotide **1–9** terminal phosphate (○), drug–DNA (×), B-DNA (△), and A-DNA (□) shifts are shown.

1979; Reinhardt & Krugh, 1977; Gorenstein, 1978; Gorenstein & Goldfield, 1984; Lai et al., 1983). The helical twist values that we have used in Figure 8 from the data of Jones and Wilson (1980) represent the difference between the normal B-DNA helical twist angle of 35.6° and the observed helical unwinding angle resulting from binding of the drug. Because of the nearest-neighbor exclusion principle (Saenger, 1984), at saturating concentrations of these drugs, only every other site has a bound drug. Only one ^{31}P signal is observed in these drug complexes (Jones & Wilson, 1980), and this must represent an average of the ^{31}P chemical shifts of phosphates at nonintercalative and intercalative sites. Technically, correction for this fast chemical exchange averaging should be made in Figure 8 by multiplying the observed perturbation of the drug–DNA ^{31}P shifts by two. This appears reasonable since in one structure where separate ^{31}P signals for the two sites are observed [poly(A)·oligo(U)–ethidium ion duplex complex (Goldfield et al., 1983)] the ^{31}P chemical shift of the phosphates in the intercalated drug duplex is shifted ~2.0 ppm downfield from that of the phosphates in the nonintercalative site. In other intercalative drug–duplex complexes where the ^{31}P signals are in slow chemical exchange, shifts of 1.5–2.5 ppm at the site of intercalation are found (Patel, 1974a,b, 1976). In two instances, ^{17}O (or ^{18}O) labeling of the phosphates at the site of intercalation has definitively identified the ^{31}P signals that are perturbed downfield upon binding the drug actinomycin D (Petersheim et al., 1984; Shah et al., 1984b).

Sequence-Specific Variation of ^{31}P Chemical Shifts in the Internal Region of the Duplex. As pointed out above, ^{31}P chemical shifts appear to vary in response to changes of helical twist (or roll angle). This correlation, however, is found largely at the ends of the duplex oligonucleotides. It appears, simply on the basis of the different ^{31}P chemical shift pattern of each region (Figures 5–7), that relief of the purine–purine clash is carried out differently for internal and terminal regions.

It is important to recall that the purine–purine minor groove clash is approximately twice as severe as that occurring in the major groove (Calladine, 1982; Fratini et al., 1982). Note in Figures 5–7 that ^{31}P shifts of phosphates at 5′-pyrimidine–purine-3′ base steps (involved in minor groove clash) resonate at lower fields than "normally" expected. On the other hand, isolated major groove clash steps appear to follow the positional relationship. Thus, the important point to emphasize is that Calladine rules predict a major perturbation in structure at the minor groove clash and an *opposite* change at adjacent base steps. These predictions on structural changes agree with our ^{31}P chemical shift data.

Different clash relief processes occur for each region of the duplex and are best established by the correlation (or lack of correlation) of ^{31}P chemical shifts with either helix twist or roll angle in the different regions of the duplex. Representative plots of each, along with the ^{31}P chemical shifts, are shown in Figures 5 and 9. As can be seen in Figure 5, the ^{31}P chemical shift pattern of the six phosphates in the terminal region follows the helical twist sum function, while that of phosphates in the internal region follows more closely the roll angle sum function (Figure 9).

Discussion

Origin of ^{31}P Chemical Shift Variations and Calladine Rules. As noted above, the possible basis for the correlation between Calladine rule sum functions and ^{31}P chemical shifts can be analyzed in terms of deoxyribose phosphate backbone distortions involved in relief of purine–purine clash. Thus, decreasing the helical twist angle, t_g, reduces the steric clashing in the minor groove in a 5′-PyPu-3′ sequence by pulling the N2 and N3 atoms of the purines further apart. As the helix unwinds (and the helix twist t_g decreases), the length of the deoxyribose phosphate backbone might be expected to decrease. These local helical changes require changes in the deoxyribose phosphate backbone angles α–ζ:

$$P^{\alpha}–O5'^{\beta}–C5'^{\gamma}–C4'^{\delta}–C3'^{\epsilon}–O3'^{\zeta}–P$$

As the helix winds or unwinds, the distance between the adjacent C4′ atoms of deoxyribose rings along an individual strand ($D_{4'4'}$) must change to reflect the stretching and contracting of the deoxyribose phosphate backbone between the two stacked base pairs. To a significant extent, these changes in the overall length of the deoxyribose phosphate backbone "tether" are reflected in changes in the P–O ester (as well as other) torsional angles.

The sequence-specific variations in the P–O (and C–O) torsional angles may provide the linkage between the Calladine rule type sequence dependent structural variations in the duplex and ^{31}P chemical shifts.

Analysis of the X-ray crystal structures (Dickerson, 1983; Dickerson & Drew, 1983; Saenger, 1984) of a B-form oligodeoxyribonucleotide (**6**) has shown that torsional angles α, β, and γ on the 5′ side of the sugar are largely constrained to values $g^-(-60°)$, $t(180°)$, $g(+60°)$, whereas significant variations are observed on the 3′ side of the deoxyribose phosphate backbone. The greatest variation in backbone torsional angles is observed for ζ (P–O3′) followed by ϵ (C3′–O3′) and then δ (C4′–C3′). It is important to note that many of these torsional angle variations are correlated, with correlation coefficients in many instances of 0.6 or greater between the different torsion angles and helical parameters (Dickerson, 1983; Dickerson & Drew, 1983; Saenger, 1984).

Torsional angle δ correlates with the sugar-puckering conformation, and the difference in δ between the two ends of a base pair correlates with the Dickerson/Calladine sum function $\sum_3$. The sugar ring constrains δ to values no smaller than 70°–85° (C3′-endo) and no larger than 140–160° (C2′-endo). Intermediate values of δ yield the other two common DNA sugar-puckering conformations [δ ~96° (O1′-endo) and ~120° (C1′-exo)]. As noted by Dickerson (Dickerson, 1983;

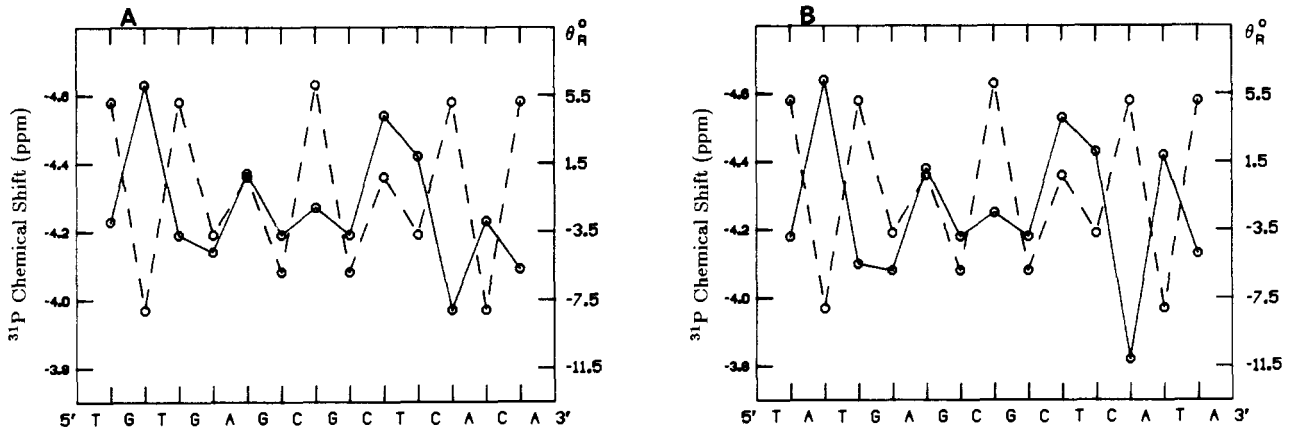

FIGURE 9: Comparison of ^{31}P chemical shifts (O—O) with helix roll angle, θ_R (O--O) as calculated from the Dickerson/Calladine sum function role for 14-mers **1** (A) and **2** (B).

Dickerson & Drew, 1983) δ, ϵ, and ζ are all correlated. At low values of δ, the phosphate P–O3′ conformation is in the low-energy g^- conformation. When the P–O3′ conformation is g^-, invariably the C–O3′ conformation (ϵ) is found to be t. This $\epsilon(t),\zeta(g^-)$ conformation is the most common backbone conformation. In this B_I (t,g) conformation, δ can vary considerably (Dickerson, 1983; Dickerson & Drew, 1983). The other most common conformation for the (ϵ,ζ) pair is the (g^-,t) or B_{II} state. A "crankshaft" motion interconverts B_I and B_{II} conformations with remarkably little overall movement of the phosphate. As δ increases to its maximum limit of ~160° in order to relieve any additional steric clash, ζ now begins to vary from −60° to −120° while ϵ largely remains fixed at trans (Dickerson, 1983; Dickerson & Drew, 1983). At a maximal value for ζ, the phosphate ester conformation can switch to the B_{II} state. It may well be significant that only terminal phosphates are observed in the B_{II} conformation in the crystal structure, (Dickerson, 1983; Dickerson & Drew, 1983) thus providing a possible rationale for the different helical adjustments that appear to be responsible for the ^{31}P chemical shift variations in different regions of the helix. It is largely this variation in δ, ϵ, and ζ that allows the sugar phosphate backbone to "stretch" or "contract" to allow for variations in the local helical twist and base-pair displacements of B-DNA. Although B-DNA winds at an average of 36°/nucleotide (~10 bp/turn), X-ray crystal structures have shown variation between 9 and 12 bp/turn. As shown by Dickerson (Dickerson, 1983; Dickerson & Drew, 1983) for phosphates in a B_I conformation, a good correlation exists between δ and the helix rotation angle r, defined between adjacent phosphates along a strand. Unwinding the double helix (increasing r and decreasing the number of base pairs (n) per turn of the helix) requires torsion about δ, ϵ, and/or ζ to open up the deoxyribose phosphate backbone to span the larger separation between stacked base pairs.

In fact, although Dickerson (Dickerson, 1983; Dickerson & Drew, 1983) suggests that the distance between adjacent phosphates (D_{pp}) along the chain does not vary greatly in response to this relief of steric strain introduced by purine–purine clash, there does appear to be a quite good correlation between D_{pp} and local helical twist parameter r, Figure 10 (correlation coefficient 0.736).

Molecular Mechanics Energy Minimization Calculation of the Sequence-Specific Variation in Deoxyribose Phosphate Backbone Conformation. Molecular mechanics and molecular dynamics calculations have not generally been able to reproduce the Calladine rule type of sequence-specific variation in the duplex geometry (Kollman et al., 1982; Singh et al., 1985).

Although the distance between the phosphates along a strand (D_{pp}) reflects the winding and unwinding of the double helix, this sequence-specific variation in the conformation of the duplex does not accurately reflect the deoxyribose phosphate backbone variation as a function of individual stacked base pairs. This distance will vary in response to local geometry changes involving *three* stacked base pairs. We have therefore chosen to introduce a new geometric parameter, the distance between adjacent C4′ atoms along an individual strand ($D_{C4'C4'}$). This distance should more accurately reflect the stretching and contracting of the deoxyribose phosphate backbone between two stacked base pairs. Using the AMBER energy-minimized, constrained d(TpG)·d(CpA) duplex dimer model, we have calculated the variation in $D_{C4'C4'}$ as a function of helix twist (Figure 11).

Decreasing the twist angle t_g from 36° to 25° reduces the steric clashing in the minor groove in a 5′-PyPu-3′ sequence by pulling the N2 and N3 atoms of the purines further apart.

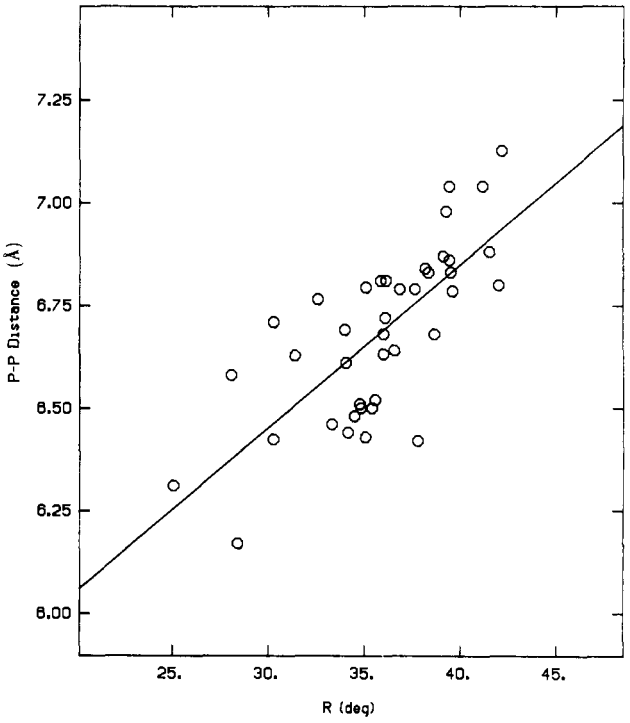

FIGURE 10: Correlation of the distance between adjacent phosphates, D_{pp}, along one strand of duplex oligonucleotide **6** and helical twist parameter r, defined by the phosphorus atoms. Line is the best least-squares fit and has no theoretical significance. All of the crystallographic data from the four 12-mer **6** structures are shown (O).

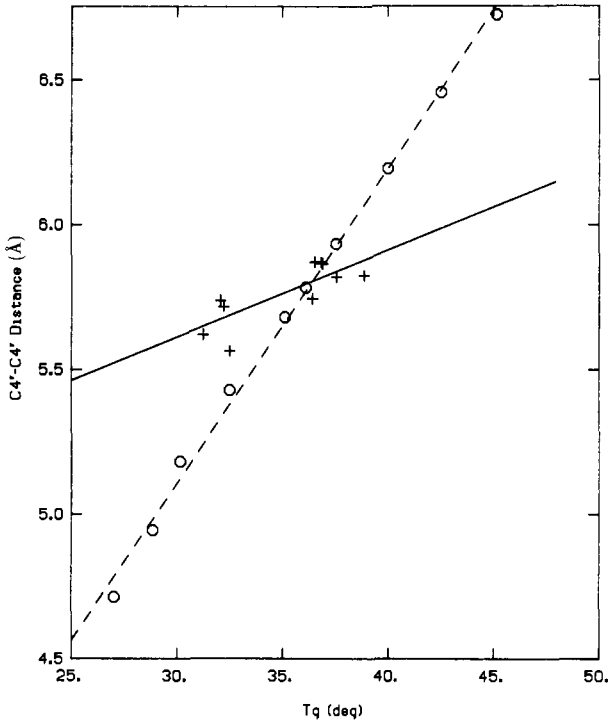

FIGURE 11: Correlation of distance between adjacent deoxyribose C4′ atoms, $D_{C4'C4'}$, along one strand of duplex oligonucleotide **6** and helical twist parameter t_g. Crystallographic data from the four 12-mer **6** structures are shown (+), as well as the AMBER, molecular mechanics energy-minimized d(TpG)·d(CpA) duplex dimer calculated results (O). The crystallographic data only includes B_I conformations, and the residue at the ends of the duplex has been eliminated. Each conformation represents the average of phosphate conformations on complementary strands and has also been end for end averaged.

As the helix unwinds, the length of the deoxyribose phosphate backbone tether is expected to decrease: the calculations suggest a decrease from ~5.8 to 4.7 Å (in contrast, the variation in D_{pp} is smaller and more complex). As the helix more tightly winds with t_g increasing to 45°, the $D_{C4'C4'}$ increases to 6.7 Å.

Significantly, the $D_{C4'C4'}$ distances obtained from the four crystal structures (Dickerson, 1983; Dickerson & Drew, 1983; Saenger, 1984) of 12-mer oligonucleotide **6** also follow a similar change as a function of t_g, as shown in Figure 11. The correlation coefficient between the crystallographically derived $D_{C4'C4'}$ distances and t_g is a quite respectable value of 0.77. While the calculated distances respond more steeply to the variation in t_g than the actual values, the trend is similar. This is reasonable since we are ignoring other helical adjustments (e.g., roll and base slide) which must also perturb the backbone length. It should be noted that only the B_I backbone conformations were included in the data of Figure 11 and the correlation breaks down if both B_I and B_{II} conformations are analyzed. Similar changes in $D_{C1'C1'}$ distances as a function of t_g are observed in the crystallographic data (R = 0.78) and the calculated geometries.

Sequence-Specific Variation of ^{31}P Chemical Shifts and Backbone Torsional Angles. These conformational changes may provide an explanation for the Calladine rule type sequence dependent variation in ^{31}P chemical shifts. As mentioned above, two of the most important parameters controlling ^{31}P chemical shifts in phosphate esters are the P–O torsional angles (in nucleic acids the α and ζ torsional angles) (Gorenstein, 1987; Gorenstein & Kar, 1975) and C–O torsional angles (β, ϵ) (Giessner-Prettre et al., 1984; Ribas-Prado et al., 1979), although the P–O torsional angle may be more important. It is thus most significant that there appears to be a strong correlation between the C3′–O3′—P–O5′ (ζ) torsion angles and ^{31}P chemical shifts in the oligomers. Using measured $J_{H3'-P}$ coupling constants [following a pulse scheme of Sklenář and Bax (Sklenář & Bax, 1987; Schroeder et al., unpublished results)] and the Karplus relationship, it is possible to calculate H3′–C3′—O3′–P torsional angles for oligonucleotide duplexes *in solution.* From these coupling constants we have calculated both C4′–C3′—O3′–P (ϵ) and C3′–O3′—P–O5′ (ζ) torsional angles. [Recall the strong coupling, R = 0.92, shown by Dickerson (Dickerson, 1983; Dickerson & Drew, 1983) between torsional angles ζ and ϵ in the crystal structure of **6**. ζ was calculated from the relationship (Dickerson, 1983; Dickerson & Drew, 1983) $\zeta = -347 - 1.22\epsilon$.] Shown in Figure 12 is a plot of the variation of both ζ and ^{31}P chemical shifts for the 12-mer sequence **6** [torsional angles for **6** were obtained from Sklenar and Bax (1987)]. The correlation coefficient between ζ (or ϵ) and ^{31}P chemical shifts for 12-mer **6** is a very good 0.90. We have also confirmed that $J_{H3'-P}$ coupling constants and ^{31}P chemical shifts are correlated for several other oligonucleotide duplexes (Schroeder et al., unpublished results), and a plot of ^{31}P chemical shifts for oligonucleotides 12-mer **6**, GT-12mer **5**, a 10-mer (dCCCGATCGGG), and 14-mer **1** vs torsional angles ζ and ϵ is shown in Figure 13. The correlation coefficient between ζ (or ϵ) and ^{31}P chemical shifts for all of the data shown in Figure 13 is 0.70.

Note that $J_{H3'-P}$ (and by inference ζ and ϵ) follows the helix twist sum function pattern only at the ends of the helix, just

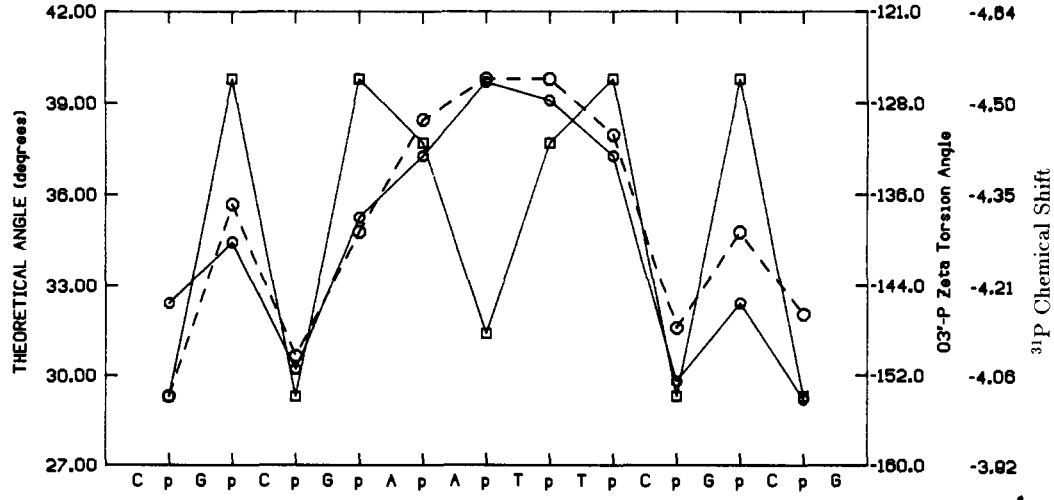

FIGURE 12: Plot of sum function calculated helix twist (□), ζ torsional angles (O--O), and ^{31}P chemical shifts (O—O) for the 12-mer **6** sequence.

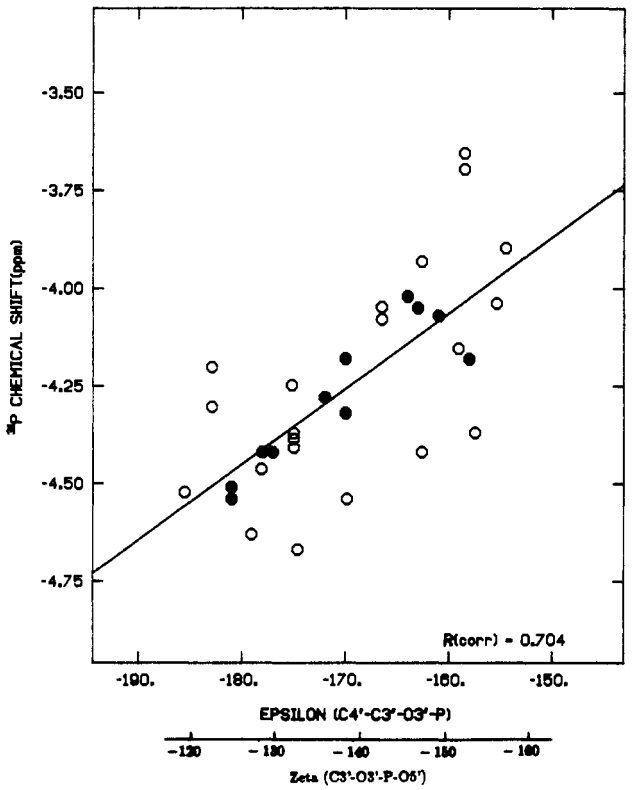

FIGURE 13: Comparison of ^{31}P chemical shifts and P–O3′ ester torsional angle ζ and C–O3′ torsional angle ϵ for 12-mer **6** (●) and GT-12mer **5**, a 10-mer (dCCCGATCGGG), and 14-mer **1** (○). ζ torsional angle calculated from reported $J_{H3'-P}$ coupling constants (Bax, private communication; Gorenstein et al., unpublished results), the calculated ϵ torsional angle from the Karplus relationship, and the correlation (Dickerson, 1983) between ϵ and ζ ($\zeta = -347 - 1.23\epsilon$).

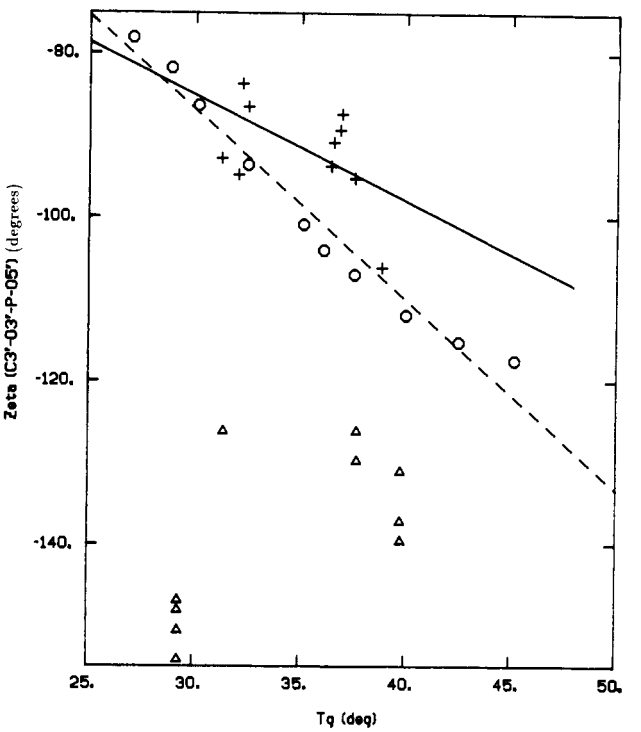

FIGURE 14: Comparison of gas-phase calculations, solution conformational data, and X-ray crystallographic data on 12-mer **6**. Plot of calculated ζ, P–O3′, torsional angles as a function of helix twist, t_g, on the basis of the AMBER, molecular mechanics energy-minimized d(TpG)·d(CpA) duplex dimer structures (○). Also shown are the ζ torsional angles derived from the X-ray crystal structures (Dickerson, 1983) of 12-mer **6** (+). The crystallographic data only include B_I conformations, and the residue at the ends of the duplex has been eliminated. Each conformation represents the average of phosphate conformations on complementary strands and has also been end-for-end averaged. The ζ torsional angles derived from the solution coupling constants (see Figure 13) are also shown (△). Lines represent the best least-squares fit of the crystal and theoretical data.

as is observed for the ^{31}P chemical shifts. This further substantiates the point we earlier made regarding the distinction between helix adjustment in response to steric clash at the ends vs the middles of the duplex. Dickerson and Calladine have shown that sequence-specific helix distortions as measured by adjustments of the bases are well represented *throughout the entire helix* by the sum function relationships (except for the residue at each end of the helix).

Dickerson has also noted that there appears to be little correlation between the helical parameters and the deoxyribose phosphate backbone torsional angles. However, analysis of the crystallographically derived backbone torsional angles for 12-mer **6** shows a modest (Figure 14) correlation between t_g and ζ ($R = -0.50$), consistent with the AMBER-calculated ζ torsional angle variations (Figure 14). No significant correlations are observed between α and ϵ and t_g, although our calculations would suggest a modest variation in ϵ. Much of the scatter in the X-ray crystallographic, torsional angle data is probably attributable to hydration and crystal-packing forces.

The calculations and data of Figures 10–14 strongly support our hypothesis that the sequence-specific variation in ^{31}P chemical shifts is largely attributable to sequence-specific variations in the helical parameters and the backbone torsional angles (at least for ζ and ϵ). Unwinding the double helix decreases $D_{C4'C4'}$, and it is largely δ, α, and ζ that vary in response to variation in t_g and $D_{C4'C4'}$ (Figures 11 and 14). Although the correlation of t_g with ζ (Figure 14) is not as good as that between δ and t_g, it appears that, on the basis of the crystal structure and the new solution conformational data for the 12-mer **6** (Figure 13), a DNA conformation with $t_g \sim 40°$ has $\zeta \sim -130°$ (or $-110°$ from the crystal data and calculations of Figure 14), $\epsilon \sim -190°$ (or $-180°$ from the crystal data and calculations), and $\alpha \sim -60°$ [α approximated from the crystal data (Dickerson, 1983; Dickerson & Drew, 1983)]. Unwinding the helix to $t_g \sim 29°$ appears to shift ζ to $-100°$ (or $-80°$ from the crystal data and calculations of Figure 14), ϵ to 170°, and α to $-50°$ (at least at the ends of the helix).

On the basis of our theoretical calculations of the variation of ^{31}P chemical shifts with P–O torsional angles (Gorenstein, 1983; Gorenstein & Kar, 1975), ^{31}P shifts could vary by ~0.4–0.6 ppm as ζ and α vary by ~10–30° in response to a chnge in the helix twist of 10–11°. It is also quite possible that C–O torsional variations are responsible for some of these ^{31}P chemical shift changes as well. Because ϵ (C–O3′) and β (C–O5′) torsional angles also vary by 10–20° over this t_g range, this could provide an additional explanation for these variations. Fortunately, as mentioned above the C–O and P–O torsional angles are highly correlated. As a cautionary note the ^{31}P chemical shifts cannot probably be theoretically calculated to this level of accuracy anyway, and any attempt to derive accurate torsional angles from the ^{31}P chemical shifts must be based upon experimentally derived correlations such as shown in Figure 13. It may well be possible that ^{31}P chemical shifts can be used to derive accurate ζ and ϵ torsional angles that can be used in restrained molecular dynamics calculations of nucleic acid structure.

Binding an intercalating drug to DNA also unwinds the duplex (Saenger, 1984) and causes a downfield shift of the ^{31}P signal (Gorenstein, 1981). This unwinding does *not* cause a further decrease in $D_{C4'C4'}$ because the deoxyribose phosphate

backbone must now bridge a base to base separation of 6.7 Å to accommodate the intercalated drug. This increase in $D_{4'4'}$ and decrease in t_g upon intercalation of a drug can be accomplished by the phosphate switching from the B_I ($\zeta = g^-$, $\alpha = g^-$) to the B_{II} conformation ($\zeta = t$, $\alpha = g^-$), and now we would expect to observe a large downfield shift ^{31}P signal. [The ^{31}P signal of a phosphate in a g^-,t B_{II} conformation is predicted to be ~1.0–1.5 ppm downfield from the g^-,g^- phosphate in the B_I conformation (Gorenstein, 1981).]

There is still considerable scatter in the data of Figures 8 and 13. As mentioned above, another factor that will affect ^{31}P chemical shifts is the degree of conformational constraint imposed by the duplex geometry. Base pairs closer to the ends of the duplex are less constrained to the stacked, base-paired geometry. This "fraying" at the ends imparts greater conformational flexibility to the deoxyribose phosphate backbone, and thus phosphates at the ends of the duplex will tend to adopt more of a mixture of g^-,g^- and g^-,t conformations. This "positional" ^{31}P chemical shift effect is presumably superimposed on the sequence-specific torsional angle adjustments.

^{31}P NMR of Polynucleotides. On the basis of the crystal structure (Viswamitra et al., 1978) of $d(AT)_2$ Klug and coworkers (Lomonossof et al., 1981) suggested that poly[d(AT)] exists in an "alternating B" conformation. Significantly the ^{31}P spectrum of poly[d(AT)] gives two signals separated by as much as 0.8 ppm depending upn salt conditions (Shindo et al., 1979). By thiophosphoryl labeling, Eckstein and Jovin (1983) were able to establish that the downfield-shifted ^{31}P signal arises from the TpA phosphates, which on the basis of an X-ray crystal model are in a more extended trans-like phosphate ester conformation. The ^{31}P signal of the ApT phosphates is quite similar to that of normal B-DNA phosphates and indeed is in a g^-,g^- conformation.

It should be noted that poly[d(AT)] in low-salt solution shows a separation of ^{31}P signals of 0.24 ppm (Shindo et al., 1979). According to our ^{31}P chemical shift/helical twist correlation, this downfield TpA phosphate signal suggests an alternating helical twist of ~32° and 36° for the TpA and ApT portions of the duplex, respectively, consistent with the X-ray studies. Similarly, the ^{31}P signal of chicken erythrocyte DNA shifts downfield by 0.2–0.3 ppm as it is converted from the B- to the A-DNA conformation (Kypr et al., 1986). A-DNA shows a t_g of ca. 32–34° in contrast to B-DNA with t_g of ca. 36°. These downfield shifts of the TpA phosphate in poly[d(AT)] and in A-DNA phosphates are thus in agreement with the stereoelectronic, torsional angle effect on ^{31}P chemical shifts.

Conclusions

Through ^{17}O labeling methodology or 2D NMR experiments it is now possible to unambiguously assign ^{31}P signals of duplex oligonucleotides up to at least 14 base pairs. An analysis of the ^{31}P chemical shifts of nine oligonucleotides suggests that certain common features are responsible for ^{31}P chemical shift variations.

(1) Homopolymer base steps not adjacent to 5′-PyPu-3′ steps will follow the positional relationship. Phosphate positions located toward the ends of the sequence will have a slightly lower field ^{31}P shift (0.2–0.4 ppm) than equivalent positions located in the central region of the sequence. Positions near the ends will likely have the lowest field ^{31}P shift of all phosphate residues. Those that are adjacent to 5′-PyPu-3′ steps will be more upfield than if predicted from the positional relationship.

(2) All 5′-PyPu-3′ base steps will be associated with a downfield ^{31}P chemical shift with respect to the positional relationship, regardless of base sequence.

(3) 5′-PuPy-3′ base steps will have corresponding ^{31}P shifts depending if the base step is isolated, adjacent to, or flanked by 5′-PyPu-3′ base steps: (a) Isolated 5′-PuPy-3′ steps will follow the phosphate positional relationship. (b) If adjacent or flanked by 5′-PyPu-3′ base steps, the associated ^{31}P chemical shift can either vary upfield or downfield depending on the actual base sequence. This ambiguity may often be resolved by application of point 4.

(4) In most instances, particularly at the ends of a duplex oligonucleotide, application of Calladine's rules (using the helical twist sum function relationship) allows a simple prediction of ^{31}P chemical shifts. Generally, ^{31}P chemical shifts of phosphates in dinucleotide units with higher helical twist values will be upfield of those with lower predicted helical twist values.

(5) Opposing phosphates on complementary strands have similar ^{31}P chemical shifts. However, complementary phosphate positions at clash steps will have a more upfield ^{31}P shift for those occurring in the 5′–3′ direction than those in the 3′–5′ direction, regardless of base sequence, position, or which groove the clash occurs. In contrast, phosphate positions at homopolymer steps will resonate more upfield at complementary positions in the 3′–5′ direction than those in the 5′–3′ direction.

(6) Finally, correlations between experimentally measured P–O and C–O torsional angles and results from molecular mechanics energy minimization calculations show that these results are consistent with the hypothesis that sequence-specific variations in ^{31}P chemical shifts are attributable to these sequence-specific changes in helical parameters (see point 4). The major structural variation responsible for these ^{31}P shift perturbations appears to be P–O and C–O backbone torsional angles which respond to changes in the local helical structure (e.g., helix twist and roll angle). Furthermore, ^{31}P chemicalshifts and $J_{H3'-P}$ coupling constants both indicate that these backbone torsional angle variations are more permissive at the ends of the double helix than in the middle.

^{31}P NMR spectroscopy therefore appears to be able to provide a powerful probe of sequence-specific structural variations along the backbone of the DNA in solution.

Acknowledgments

The contributions of R. Powers and R. Santini are much appreciated.

References

Anderson, J. E., Ptashne, M., & Harrison, S. C. (1985) *Nature (London) 316*, 596–600.

Anderson, J. E., Plashne, M., & Harrison, S. C. (1987) *Nature (London) 326*, 846–852.

Assa-Munt, N., & Kearns, D. R. (1984) *Biochemistry 23*, 791.

Broido, M. A., Zon, G., & James, T. L. (1984) *Biochem. Biophys. Res. Commun. 119*, 663–670.

Calladine, C. R. (1982) *J. Mol. Biol. 161*, 343–352.

Calladine, C. R., & Drew, H. R. (1984) *J. Mol. Biol. 178*, 773–782.

Cheng, D. M., Kan, L.-S., Miller, P. S., Leutzinger, E. E., & Ts'o, P. O. P. (1982) *Biopolymers 21*, 697.

Cheng, D. M., Kan, L., & Ts'o, P. O. P. (1987) *Phosphorus NMR in Biology* (Burt, C. T., Ed.) pp 135–147, CRC, Boca Raton, FL.

Clore, G. M. Gronenborn, A. M., Brunger, A. T., & Karplus, M. (1985) *J. Mol. Biol. 186*, 435–455.

Connolly, B. A., & Eckstein, F. (1984) *Biochemistry 23*, 5523–5527.

Costello, A. J. R., Glonek, T., & Van Wazer, J. R. (1976) *J. Inorg. Chem. Soc. 15*, 972–974.

Dickerson, R. E. (1983) *J. Mol. Biol. 166*, 419–441.

Dickerson, R. E., & Drew, H. R. (1981) *J. Mol. Biol. 149*, 761–786.

Dickerson, R. E., & Drew, H. R. (1983) *J. Mol. Biol. 149*, 761–786.

Eckstein, F., & Jovin, T. M. (1983) *Biochemistry 22*, 4546–4550.

Feigon, J., Leupin, W., Denny, W. A., & Kearns, D. R. (1983a) *Biochemistry 22*, 5930–5942.

Feigon, J., Leupin, W., Denny, W. A., & Kearns, D. R. (1983b) *Biochemistry 22*, 5943–5951.

Fratini, A. V. Kopka, M. L., Drew, H. R., & Dickerson, R. E. (1982) *J. Biol. Chem. 257*, 14686–14707.

Frechet, D., Cheng, D. M., Kan, L.-S., & Ts'o, P. O. P. (1983) *Biochemistry 22*, 5194–5200.

Fu, J. M., Schroeder, S. A., Jones, C. R., Santini, R., & Gorenstein, D. G. (1988) *J. Magn. Reson. 77*, 577–582.

Giessner-Prettre, C., Pullman, C., Borer, B., Kan, L. S., & Ts'o, P. O. P. (1976) *Biopolymers 15*, 2277.

Giessner-Prettre, C., Pullman, B., Ribas-Prado, F., Cheng, D. M., Iuorno, V., & Ts'o, P. O. P. (1984) *Biopolymers 23*, 377.

Goldfield, E. M., Luxon, B. A., Bowie, V., & Gorenstein, D. G. (1983) *Biochemistry 22*, 3336.

Gorenstein, D. G. (1978) *Jerusalem Symposium, NMR in Molecular Biology* (Pullman, B., Ed.) pp 1–15, D. Reidel, Dordrecht, The Netherlands.

Gorenstein, D. G. (1981) *Annu. Rev. Biophys. Bioeng. 10*, 355.

Gorenstein, D. G. (1983) *Prog. Nucl. Magn. Reson. Spectrosc. 161*, 1–98.

Gorenstein, D. G. (1984) *Phosphorus-31 NMR: Principles and Applications* (Gorenstein, D. G., Ed.) Academic, New York.

Gorenstein, D. G. (1987) *Chem. Rev. 87*, 1047–1077.

Gorenstein, D. G., & Kar, D. (1975) *Biochem. Biophys. Res. Commun. 65*, 1073–1080.

Gorenstein, D. G., & Findlay, J. B. (1976) *Biochem. Biophys. Res. Commun. 72*, 640.

Gorenstein, D. G., & Kar, D. (1977) *J. Am. Chem. Soc. 99*, 672–677.

Gorenstein, D. G., & Goldfield, E. M. (1984) *Phosphorus-31 NMR: Principles and Applications* (Gorenstein, D. G., Ed.) Academic, New York.

Gorenstein, D. G., Findlay, J. B., Momii, R. K., Luxon, B. A., & Kar, D. (1976) *Biochemistry 15*, 3796–3803.

Gorenstein, D. G., Luxon, B. A., & Findlay, J. B. (1977) *Biochim. Biophys. Acta 475*, 184–190.

Gorenstein, D. G., Schroeder, S., Miyasaki, M., Fu, J., Jones, C., Roongta, V., & Abuaf, P. (1987) *Phosphorus Sulfur 30*, 567–570.

Gorenstein, D. G., Schroeder, S. A., Miyasaki, M., Fu, J. M., Roongta, V., Abuaf, P., Chang, A., & Yang, J. C. (1987) *Biophosphates and Their Analogues—Synthesis, Structure, Metabolism and Activity* (Bruzik, K. S., & Stec, W. J., Eds.) pp 487–502, Elsevier, Amsterdam.

Hare, D. R., Wemmer, D. E., Chou, S. H., Drobny, G., & Reid, B. (1983) *J. Mol. Biol. 171*, 319.

Hare, D., Shapiro, L., & Patel, D. J. (1986) *Biochemistry 25*, 7456–7464.

Hochschild, A., & Ptashne, M. (1986) *Cell (Cambridge, Mass.) 44*, 681.

James, T. L. (1984) *Phosphorus-31 NMR: Principles and Applications* (Gorenstein, D. G., Ed.) pp 349–400, Academic, New York.

Jones, R. L., & Wilson, W. D. (1980) *J. Am. Chem. Soc. 102*, 7776–7778.

Kearns, D. R. (1984) *Crit. Rev. Biochem. 15*, 237–290.

Klug, A., Viswamitra, M. A., Kennard, O., Shakked, Z., & Steitz, T. A. (1979) *J. Mol. Biol. 131*, 669–680.

Kollman, P., Keepers, J. W., & Weiner, P. (1982) *Biopolymers 21*, 2345.

Kypr, J., Sklenar, V., & Vorlic-Kova, M. (1986) *Biopolymers 25*, 1803–1812.

Lai, K., Gorenstein, D. G., & Goldfield, E. M. (19883) *Bull. Magn. Reson. 5*, 253.

Lai, K., Shah, D. O., Derose, E., & Gorenstein, D. G. (1984) *Biochem. Biophys. Res. Commun. 121*, 1021.

Lefevre, J., Lane, A. N., & Jardetzky, O. (1987) *Biochemistry 26*, 5076–5090.

Lerner, D. B., & Kearns, D. R. (1980) *J. Am. Chem. Soc. 102*, 7612–7613.

Levitt, M. (1978) *Proc. Natl. Acad. Sci. U.S.A. 75*, 640–644.

Lomonossof, G. P., Butler, P. J. G., & Klug, A. (1981) *J. Mol. Biol. 149*, 745–760.

Martin, K., & Schleif, R. F. (1986) *Proc. Natl. Acad. Sci. U.S.A. 83*, 3654.

McClarin, J. A., Frederick, C. A., Wang, B. C., Greene, P., Boyer, H. W., Grable, J., & Rosenberg, J. M. (1986) *Science (Washington, D.C.) 234*, 1526–1541.

Nilges, M., Clore, G. M., Gronenborn, A. M., Brunger, A. T., Karplus, M., & Nilsson, L. (1987a) *Biochemistry 26*, 3718–3733.

Nilges, M., Clore, G. M., Gronenborn, A. M., Piel, N., & McLaughlin, L. W. (1987b) *Biochemistry 26*, 3734–3744.

Ott, J., & Eckstein, F. (1985a) *Biochemistry 24*, 2530–2535.

Ott, J., & Eckstein, F. (1985b) *Nucleic Acids Res. 13*, 6317–6330.

Patel, D. J. (1974a) *Biochemistry 13*, 2388–2395.

Patel, D. J. (1974b) *Biochemistry 13*, 2396–2402.

Patel, D. J. (1979) *Acc. Chem. Res. 12*, 118.

Patel, D. J., Pardi, A., & Itakura, K. (1982) *Science (Washington, D.C.) 216*, 581.

Patel, D. J., Kozlowski, S. A., & Bhatt, R. (1983) *Proc. Natl. Acad. Sci. U.S.A. 80*, 3908–3912.

Patel, D. J., Shapiro, L., & Hare, D. (1987) *Biophys. Chem. 16*, 423–454.

Petersheim, M., Mehdi, S., & Gerlt, J. A. (1984) *J. Am. Chem. Soc. 106*, 439–440.

Reinhardt, C. G., & Krugh, T. R. (1977) *Biochemistry 16*, 2890–2895.

Ribas-Prado, F., Giessner-Prettre, C., Pullman, B., & Daudey, J.-P. (1979) *J. Am. Chem. Soc. 101*, 1737.

Richmond, T. J., Finch, J. T., Rushton, B., Rhodes, D., & Klug, A. (1985) *Nature (London) 311*, 532.

Riggs, A. D., Lin, S.-Y., & Wells, R. D. (1972) *Proc. Natl. Acad. Sci. U.S.A. 69*, 761–764.

Rinkel, L. J., van der Marel, G. A., van Boom, J. H., & Altona, C. (1987) *Eur. J. Biochem. 163*, 275–286.

Saenger, W. (1984) *Principles of Nucleic Acid Structure*, Springer-Verlag, New York.

Scheek, R. M., Boelens, R., Russo, N., Van Boom, J. H., & Kaptein, R. (1984) *Biochemistry 23*, 1371–1376.

Scheffler, I. E., Elson, E. L., & Baldwin, R. L. (1968) *J. Mol. Biol. 36*, 291–304.

Schroeder, S., Jones, C., Fu, J., & Gorenstein, D. G. (1986) *Bull. Magn. Reson. 8*, 137–146.

Schroeder, S., Fu, J., Jones, C., & Gorenstein, D. G. (1987) *Biochemistry 26*, 3812–3821.
Seeman, N. C., Rosenberg, J. M., Suddath, F. L., Park Kim, J. J., & Rich, A. (1976) *J. Mol. Biol. 104*, 142–143.
Shah, D. O., Lai, K., & Gorenstein, D. G. (1984a) *Biochemistry 23*, 6717–6723.
Shah, D. O., Lai, K., & Gorenstein, D. G. (1984b) *J. Am. Chem. Soc. 106*, 4302.
Shindo, H., Simpson, R. T., & Cohen, J. S. (1979) *J. Biol. Chem. 254*, 8125.
Singh, U. C., Weiner, S. J., & Kollman, P. (1985) *Proc. Natl. Acad. Sci. U.S.A. 82*, 755.
Sklenář, V., & Bax, A. (1987) *J. Am. Chem. Soc. 109*, 7525.
Sklenář, V., Miyashiro, H., Zon, G., Miles, H. T., & Bax, A. (1986) *FEBS Lett. 208*, 94–98.
Sundaralingam, M. (1969) *Biopolymers 7*, 821–860.
Viswamitra, M. A., Kennard, O., Shakked, Z., Jones, D. G., Sheldrick, G. M., Salisbury, S., & Falvello, L. (1978) *Nature (London) 273*, 687–690.
Weiner, P. K., & Kollman, P. A. (1981) *J. Comput. Chem. 2*, 287.
Wemmer, D. E., & Reid, B. R. (1985) *Ann. Rev. Phys. Chem. 36*, 105–137.

Oligonucleotide *N*-Alkylphosphoramidates: Synthesis and Binding to Polynucleotides†

Alfred Jäger, Mark J. Levy,‡ and Sidney M. Hecht*
Departments of Chemistry and Biology, University of Virginia, Charlottesville, Virginia 22901
Received April 4, 1988; Revised Manuscript Received June 1, 1988

ABSTRACT: A few different methods for the preparation of oligonucleotide *N*-alkylphosphoramidates were compared directly. One of these, involving the use of protected nucleoside phosphites as building blocks, provided the requisite *N*-alkylphosphoramidates via oxidation of the intermediate dinucleoside methyl phosphites with iodine in the presence of the appropriate alkylamine. This method was found to have several attractive features, including the use of building blocks identical with those employed for the synthesis of DNA and compatibility with procedures and instruments employed for the stepwise synthesis of oligonucleotides by solution and solid-phase methods. This procedure was used to make several di-, tri-, and tetranucleotide *N*-alkylphosphoramidates derived from deoxyadenosine and thymidine; alkyl substituents included *N*,*N*-dimethyl, *N*-butyl, *N*-octyl, *N*-dodecyl, and *N*-(5-aminopentyl). The aminoalkyl derivative of d(TpT) (**24**) was used to demonstrate the feasibility of introducing an intercalative agent to the alkylphosphoramidate moiety of such derivatives. The oligonucleotide *N*-alkylphosphoramidates were separated into their component diastereomers and characterized structurally by a number of techniques including circular dichroism, high-field ^{1}H NMR spectroscopy, FAB mass spectrometry, and enzymatic digestion to authentic nucleosides and nucleotides. Physicochemical characterization of several di- and trinucleotide alkylphosphoramidates revealed that the adenine nucleotide analogues formed stable complexes with poly(thymidylic acid). The stabilities of these complexes were found to increase with increasing chain length of the *N*-alkylphosphoramidate substituents. The finding that *N*-alkylphosphoramidate substituents can enhance the binding of certain oligonucleotides to their complementary polynucleotides suggests the existence of a novel source of polynucleotide affinity.

The preparation of oligonucleotides containing modified phosphodiester linkages is of current interest as a source of sequence-specific nucleic acid probes (Miller et al., 1981; Letsinger & Schott, 1981; Asseline et al., 1984; Chu & Orgel, 1985; Dreyer & Dervan, 1985; Thuong et al., 1987). Nucleoside phosphoramidates have been prepared previously by several procedures involving both tri- and pentavalent phosphorous intermediates. These have included the condensation of nucleoside phosphate diesters with amines in the presence of triphenylphosphine–CCl_4 (Appel 1975; Stec, 1983), nucleophilic substitution of nucleoside phosphate triesters with alkylamines (Meyer et al., 1973; Juodka & Smrt, 1974; Letsinger et al., 1986), addition of alkyl and aryl azides to phosphites (Cramer et al., 1972; Letsinger & Schott, 1981), as well as the oxidation of intermediate nucleoside phosphites (Nemer & Ogilvie, 1980a,b) or nucleoside hydrogen phosphonate diesters (Froehler, 1986) with iodine in the presence of alkylamines.

Presently, we describe experiments that define the scope and utility of such transformations for the preparation of oligonucleotide phosphoramidates, by both solution and solid-phase techniques. Also described is chromatographic resolution and analysis of the formed diastereomers and their analysis by spectral and degradative techniques.

The association of a series of diadenosine *N*-alkylphosphoramidates with poly(thymidylic acid) was characterized by measurement of T_m and hypochromicity values, as well as by determination of the stoichiometry of association. These measurements indicated that the *N*-alkyl groups promoted the binding of the diadenosine *N*-alkylphosphoramidate derivatives to poly(T) and that affinity increased with increasing alkyl

†This work was supported in part by USPHS Research Grant GM27815. A.J. was supported by a fellowship from Smith Kline & French Laboratories.
‡NIH National Research Service Awardee, National Cancer Institute.

0006-2960/88/0427-7237$01.50/0